NASA CONTRACTOR REPORT

NASA CR-677

NASA CR-677

ON THE RADIATION OF A MAGNETIC LINE SOURCE EXCITED CYLINDER THROUGH AN AXIALLY SLOTTED PLASMA SHEATH

by Andrejs Olte

Prepared by
UNIVERSITY OF MICHIGAN
Ann Arbor, Mich.
for

NATIONAL AERONAUTICS AND SPACE ADMINISTRATION • WASHINGTON, D. C. • JANUARY 1967

NASA CR-677

ON THE RADIATION OF A MAGNETIC LINE SOURCE EXCITED CYLINDER

THROUGH AN AXIALLY SLOTTED PLASMA SHEATH

By Andrejs Olte

ABSTRACT

A plasma sheath encloses a perfectly conducting cylinder with a time
harmonic magnetic line source on its surface. The plasma sheath has an in-
finite axial slot. A singular integral equation is formulated for the
electric plasma current whose solution unfortunately was not found. However,
some approximations for the current of underdense plasma are suggested to
predict the effect of the slotted plasma sheath on the cylinder radiation.
For overdense plasma the slot may support traveling waves which transport
power from the source to the external space. Radiation is calculated
through a narrow parallel face slot that supports the propagation only of
the lowest order mode. It is shown that the radiation in the forward
direction is comparable to the case of no plasma sheath.

TABLE OF CONTENTS

LIST OF FIGURES

I
INTRODUCTION

In this report we consider a magnetic line source excited perfectly conducting cylinder radiation through a uniform plasma sheath. The fields are of two-dimensional nature. Taking the z-axis of a cartesian coordinate system (x,y,z) coincident with the axis of the perfectly conducting cylinder the electric field components $E_x(x,y)$ and $E_y(x,y)$, and the magnetic field component $H_z(x,y)$ are the only ones induced by the magnetic line source.

As is well known the plasma sheath very strongly inhibits the radiation of an antenna when the plasma frequency sufficiently exceeds the frequency of the electromagnetic field. Opening a slot in the plasma sheath by depressing the plasma frequency below the field frequency, for example by material additives, may go some distance towards re-establishing some of the desirable antenna characteristics. Theoretically to establish some of these possibilities for a cylindrical configuration is the object of this report.

In the second chapter we derive a field representation in which the magnetic field due to the currents induced in the plasma by the primary antenna field (i.e., the field without the cylindrical plasma sheath present) is obtained. On the basis of this representation we obtain a two-dimensional singular integral equation for the electric plasma current under the assumption that the current satisfies the Ohm's law. A solution of the integral equation was not found. However, some approximate distributions of the electrical plasma current are suggested for an underdense plasma sheath which may be used to calculate the effect of the plasma sheath (slotted and un-slotted) on the free space radiation.

When the plasma is sufficiently overdense the electromagnetic fields hardly penetrate the plasma sheath and hence the plasma slot may be viewed as a waveguide that couples the source to the free space. A parallel face slot then may be considered as a parallel plate plasma waveguide. The Transverse Magnetic (TM) modes in such a waveguide are of a type matching the fields of our problem. We utilize the lowest order TM mode in a slot centered above the magnetic line source in a plasma sheath closely fitting the cylinder and calculate the radiation in the free space. These derivations and calculations are carried out in Chapter III .

The fourth (and last) chapter presents the conclusions of the study. Some of the very elementary derivations are relegated to the appendices.

The problem taken up in this report is a generalization of the one considered by Olte, et.al., in a 1964 Radiation Laboratory Report as well as in a paper by Olte (1965). In that study the slotted plasma sheath was considered thin, but having very high electron density, and being concentric with the antenna cylinder. In the analytical formulation the sheath was replaced by a perfectly conducting shell, thus simplifying the analytical difficulties to a large extent.

In these problems the total magnetic field is entirely tangential to the plasma sheath, slotted or un-slotted. An electric line source (of course not on the surface of a perfectly conducting cylinder), replacing the magnetic one, generates an electric field entirely tangential to the plasma sheath. This type of polarization was considered by Olte (1965, 1966) in which the electric line source was at the center of a cylindrical plasma

2

sheath with infinite axial slot.

The rationalized system of units are being used. The time dependence $\exp(j\omega t)$ is being suppressed in all formulas.

II

INTEGRAL EQUATION APPROACH

2.1 Introduction

When a plasma sheath encloses a radiating antenna the changes in the
field result from the induced plasma current radiating in the presence of
the antenna. When the antenna is a perfectly conducting cylinder excited
by a magnetic line source then the induced current in the plasma sheath
radiates in the presence of a perfectly conducting cylinder. From the
vector Green's theorem and the magnetic Green's function of the perfectly
conducting cylinder we derive a representation for the magnetic field
change when the cylinder is enclosed by a cylindrical plasma sheath of
arbitrary cross-section, but uniform density. Assuming that Ohm's law holds
for the plasma, one obtains a two dimensional singular integral equation
for the current of the plasma sheath. However, we could not solve it. In
the second part of the chapter we propose some approximate representations
for the plasma current, more or less as physical assumptions. In the case
of a concentric cylindrical plasma sheath with a wedge slot we give the
analytic form of the far-zone magnetic field.

2.2 Various Integral Representations of the Fields and a Singular Integral Equations for the Plasma Sheath Current

We show the configuration of the problem in Fig. 2.1. The cylinder of
radius a is assumed to be perfectly conducting and excited by a magnetic
line source of V volts at the position (x_s, y_s) of the cylinder surface, the
time dependence $e^{j\omega t}$ being suppressed. The cylinder is enclosed by a cylin-
drical plasma sheath of arbitrary cross-section A_p. The curve bounding

4
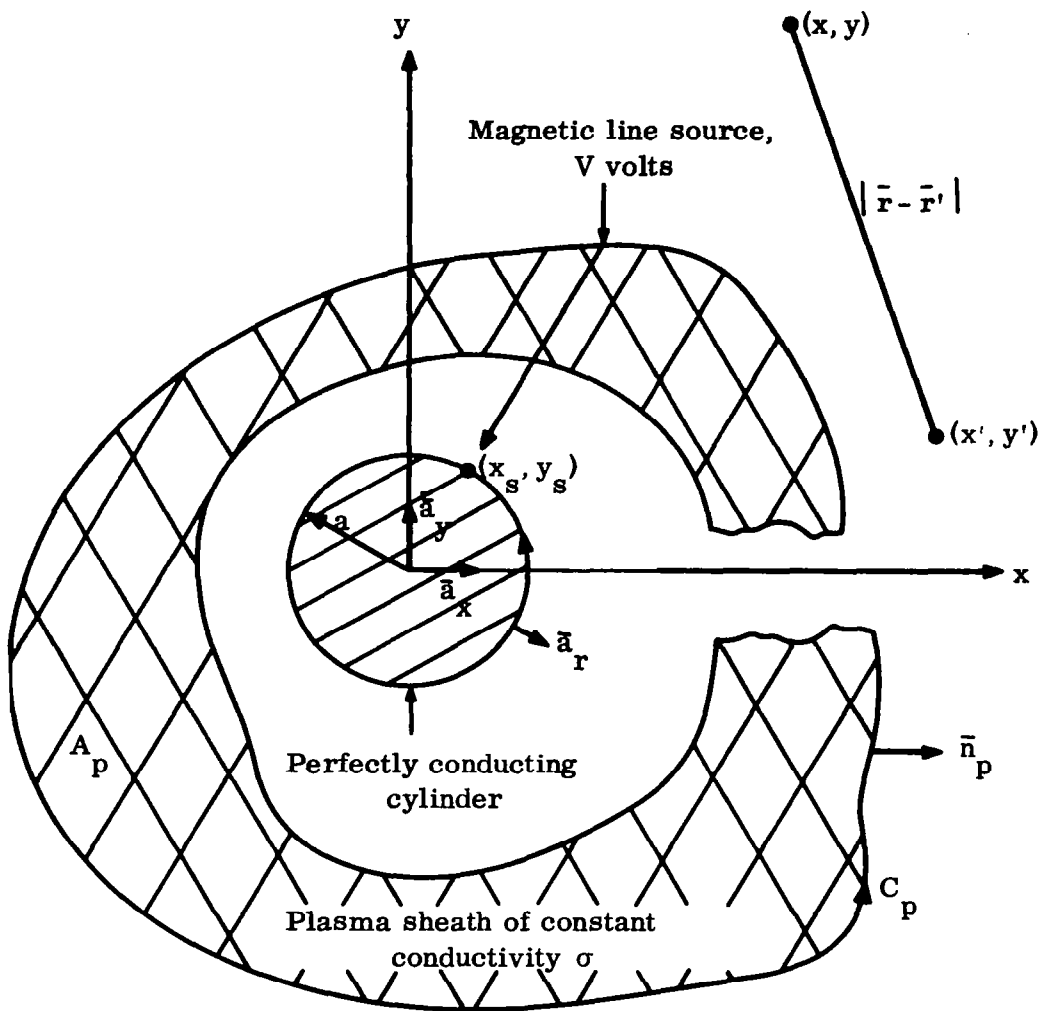
FIG. 2.1: MAGNETIC LINE SOURCE EXCITED CYLINDER ENCLOSED BY
A PLASMA SHEATH.

A_p is denoted by C_p, the positive sense as indicated. We take the plasma conductivity to be σ; permittivity and permeability are taken to be those of free space, respectively ϵ_o and μ_o.

Because a magnetic line source excites the two-dimensional structure we have

$$\bar{H} = \bar{a}_z H_z(x',y') \; ; \; \bar{E}(x',y')\cdot\bar{a}_z = \bar{i}(x',y')\cdot\bar{a}_z = 0, \qquad (2\text{-}1)$$

where $\bar{a}_z = \bar{a}_x \times \bar{a}_y$. This special nature of the vector fields will always be understood in our subsequent vector calculations. The induced fields will satisfy the Maxwell's equations

$$\nabla' \times \bar{E} = -\, j\omega\mu_o \bar{H} \qquad (2\text{-}2)$$

$$\nabla' \times \bar{H} = \bar{i} + j\omega\epsilon_o \bar{E} \qquad (2\text{-}3)$$

$$\bar{i} = 0, \quad \text{in free space}, \qquad (2\text{-}4)$$

$$\bar{i} = \sigma\bar{E}, \quad \text{in plasma.} \qquad (2\text{-}5)$$

From (2-2) and (2-3) we have

$$\nabla' \times \nabla' \times \bar{H} = k_o^2 \bar{H} + \nabla' \times \bar{i} . \qquad (2\text{-}6)$$

For the purpose of using in our derivation the two-dimensional vector Green's theorem,

$$\iint_A [\bar{H} \cdot \nabla' \times \nabla' \times \bar{H}^{(m)} - \bar{H}^{(m)} \cdot \nabla' \times \nabla' \times \bar{H}] \, dx'dy' =$$

$$\oint_C [\bar{H}^{(m)} \times \nabla' \times \bar{H} - \bar{H} \times \nabla' \times \bar{H}^{(m)}] \cdot \bar{n} \, d\ell' \quad , \qquad (2\text{-}7)$$

we introduce at (x,y) a magnetic line source of amplitude I_m and require that the fields of it satisfy

$$\nabla' \times \bar{H}^{(m)} = j\omega\epsilon_o \, \bar{E}^{(m)} \qquad (2\text{-}8)$$

$$\nabla' \times \bar{E}^{(m)} = -j\omega\mu_o \, \bar{H}^{(m)} - I_m \, \bar{a}_z \delta(|\bar{r}-\bar{r}'|) \qquad (2\text{-}9)$$

with

$$\bar{a}_r \times \bar{E}^{(m)} = 0 \quad \text{at} \ (x')^2 + (y')^2 = a^2 \quad . \qquad (2\text{-}10)$$

That is to say, $\bar{E}^{(m)}$ and $\bar{H}^{(m)}$ are the fields due to a magnetic line source in the presence of a perfectly conducting cylinder of radius a.

Applying (2-7) to the plasma sheath and to the free space separately and then adding the results, we obtain, after reducing the expressions by applying the boundary conditions,

$$I_m \bar{H} \cdot \bar{a}_z = \oint_{C_a} \bar{H}^{(m)} \times \bar{E} \cdot \bar{a}_r \, d\ell' - \frac{1}{j\omega\epsilon_o} \iint_{A_p} (\nabla' \times \bar{i}) \cdot \bar{H}^{(m)} dx'dy'$$

$$- \frac{1}{j\omega\epsilon_o} \oint_{C_p} \bar{H}^{(m)} \times \bar{i} \cdot \bar{n}_p \, d\ell' \quad . \qquad (2\text{-}11)$$

By transforming the coordinates (x', y', z') to the circular coordinate
system (r', φ', z') the integral

$$\oint_{C_a} \bar{H}^{(m)}(x,y;x',y') \times \bar{E}(x',y') \cdot \bar{a}_r d\ell' =$$

$$-\int_{o}^{2\pi} H_z^{(m)}(x,y;r' \cos \varphi', r' \sin \varphi') E_{\varphi'}(a,\varphi') a d\varphi' . \qquad (2\text{-}12)$$

The tangential electric field on the surface of the cylinder due to the
magnetic line source V is given by

$$E_{\varphi'}(a,\varphi') = -V \frac{\delta(\varphi_s - \varphi)}{a} \qquad (2\text{-}13)$$

and hence from (2-12)

$$\oint_{C_a} \bar{H}^{(m)} \times \bar{E} \cdot \bar{a}_r d\ell' = V H_z^{(m)}(x,y;x_s,y_s) \qquad (2\text{-}14)$$

From the reciprocity theorem we see that one can identify the form of
(2-14) from (A-8), i.e. in the circular coordinate system

$$\oint_{C_a} \frac{1}{I_m} \bar{H}^{(m)} \times \bar{E} \cdot \bar{a}_r d\ell' =$$

$$j \frac{k_o V}{2\pi a \omega \mu_o} \sum_{n=0}^{\infty} c_n \frac{H_n^{(2)}(k_o r)}{H_n^{(2)'}(k_o a)} \cos n (\varphi - \varphi_s) \equiv H_z^{(0)}(\bar{r};\bar{r}_s) .$$

$$(2\text{-}15)$$

In the subsequent discussion we will represent by $H_z^{(0)}$ the magnetic field for no plasma sheath, i.e., $\sigma = 0$.

In appendix A we have already solved for $\bar{H}^{(m)}$ in the circular coordinate system. From (A-5) we obtain

$$\frac{1}{I_m} \bar{H}^{(m)} = \bar{a}_z \frac{k_o^2}{4\omega\mu_o} \left\{ - H_o^{(2)}(k_o|\bar{r} - \bar{r}'|) + \sum_{n=0}^{\infty} c_n \frac{J_n'(k_o a)}{H_n^{(2)'}(k_o a)} H_n^{(2)}(k_o r')H_n^{(2)}(k_o r) \cos n\,(\varphi-\varphi') \right\} .$$

(2-16)

We define a function

$$G(\bar{r};\bar{r}') \equiv \frac{1}{4j} \left\{ - H_o^{(2)}(k_o|\bar{r} - \bar{r}'|) + \sum_{n=0}^{\infty} c_n \frac{J_n'(k_o a)}{H_n^{(2)'}(k_o a)} H_n^{(2)}(k_o r')H_n^{(2)}(k_o r) \cos n\,(\varphi-\varphi') \right\}$$

(2-17)

and thus

$$\frac{1}{j\omega\epsilon_o I_m} \bar{H}^{(m)} = \bar{a}_z\, G(\bar{r};\bar{r}')$$

(2-18)

Applying (2-16) and (2-18) we re-write (2-11) as

$$\bar{H}(\bar{r}) = \bar{a}_z H_z^{(0)}(\bar{r};\bar{r}_s) - \iint\limits_{A_p} [\nabla' \times \bar{i}(\bar{r}')]\, G(\bar{r};\bar{r}')\, dx'dy'$$

$$+ \bar{a}_z \oint\limits_{C_p} G(\bar{r};\bar{r}')\bar{i}(\bar{r}')(\bar{a}_z \times \bar{n}_p)\, d\ell' .$$

(2-19)

9

The first term on the r.h.s. of (2-19), as already mentioned, is the magnetic field from a magnetic line source on the perfectly conducting cylinder radiating in the free space. The two remaining terms come from the currents in the plasma induced by the primary source. In particular, the curl of the electric plasma current and the tangential component of the current on the plasma boundary contribute to the magnetic field $\bar{H}(\bar{r})$.

We may eliminate the surface integral in (2-19) via the Stokes's Theorem. Substituting

$$\oint_{C_p} [G(\bar{r};\bar{r}')\bar{i}(\bar{r}')] \cdot (\bar{a}_z \times \bar{n}_p) d\ell'$$

$$= \iint_{A_p} \nabla' \times [G(\bar{r};\bar{r}')\bar{i}(\bar{r}')] \cdot \bar{a}_z dx' dy'$$

$$= \iint_{A_p} \left\{ \nabla' G(\bar{r};\bar{r}') \times \bar{i}(\bar{r}') + G(\bar{r};\bar{r}')\nabla' \times \bar{i}(\bar{r}') \right\} \cdot \bar{a}_z dx' dy' \quad .$$

$$(2\text{-}20)$$

in (2-19) we have

$$\bar{H}(\bar{r}) = \bar{a}_z H_z^{(0)}(\bar{r};\bar{r}_s) + \iint_{A_p} \nabla' G(\bar{r};\bar{r}') \times \bar{i}(\bar{r}') dx' dy' \quad . \qquad (2\text{-}21)$$

Taking the curl of the last representation and noting that

$$\nabla \times \bar{H}(\bar{r}) = \bar{i}(\bar{r}) + j\omega\epsilon_o \bar{E}(\bar{r}) \quad , \quad \text{from (2-3),} \qquad (2\text{-}22)$$

10

$$\nabla \times [\bar{a}_z H_z^{(0)}(\bar{r};\bar{r}_s)] = j\omega\epsilon_o \bar{E}^{(0)}(\bar{r};\bar{r}_s), \text{ from (2-8)}, \qquad (2\text{-}23)$$

$$\nabla \times [\nabla' G(\bar{r};\bar{r}') \times \bar{i}(\bar{r}')] =$$

$$- i(\bar{r}') \cdot \nabla'\nabla' G(\bar{r};\bar{r}') + \bar{i} \nabla'^2 G(\bar{r};\bar{r}') , \qquad (2\text{-}24)$$

(since $\nabla = -\nabla'$) and

$$\nabla'^2 G(\bar{r};\bar{r}') = -k_o^2 G(\bar{r};\bar{r}') + \delta(|\bar{r}-\bar{r}'|) \qquad (2\text{-}25)$$

we obtain at point $(\bar{r})$ in the plasma

$$\bar{E}(\bar{r}) = \bar{E}^{(0)}(\bar{r};\bar{r}_s) - \frac{1}{j\omega\epsilon_o} \iint\limits_{A_p} [\bar{i}(\bar{r}') \cdot \nabla'\nabla' + k_o^2 \bar{i}] G(\bar{r};\bar{r}') dx' dy'. \qquad (2\text{-}26)$$

If the Ohm's law holds for the plasma, then

$$\bar{i}(\bar{r}) = \sigma \bar{E}(r) \qquad (2\text{-}27)$$

and from (2-26) we obtain an integral equation

$$\bar{i}(\bar{r}) + \frac{\sigma}{j\omega\epsilon_o} \iint\limits_{A_p} [\bar{i}(\bar{r}') \cdot \nabla'\nabla' + k_o^2 \bar{i}(\bar{r}')] G(\bar{r};\bar{r}') dx' dy' =$$
$$\sigma \bar{E}^{(0)}(\bar{r};\bar{r}_s) \quad . \qquad (2\text{-}28)$$

11

It is a singular integral equation since the integral exists only in a "principal value" sense. Hence any perturbation scheme in spite of the free term does not exist, nor is any exact solution in evidence.

2.3 Some Approximate Solutions

Since the integral equation (2-28) for the plasma current is not readily solvable we have to propose some approximate representations for the plasma current in order to compute the effect of the slotted plasma sheath on the antenna fields from (2-21). For plasma frequency sufficiently below the radio frequency we may take

$$\bar{i}(\bar{r}) \simeq \sigma \bar{E}^{(0)}(\bar{r};\bar{r}_s) \quad , \tag{2-29}$$

i.e., the current density is the antenna electric field in the free space multiplied by the plasma conductivity. This approximation is equally valid for arbitrary plasma sheath cross-section.

When the plasma sheath is a cylindrical shell with an axial slot a better approximation is possible. The basis of this approximation is the plasma current obtained in Appendix B for the un-slotted case of a cylindrical plasma sheath that is concentric with the antenna cylinder. In vector form we denote this current by

$$\bar{i}_0(\bar{r}) = \bar{a}_r i_r(r,\varphi) + \bar{a}_\varphi i_\varphi(r,\varphi) \tag{2-30}$$

where (B-12) and (B-10), respectively, define the scalar components of the current. This current can be used to predict the field for arbitrary slot

cross-section A_s. It is convenient then to transform (2-21) so that the integral is over A_s. Thus since

$$\bar{H}(\bar{r}) \simeq \bar{a}_z \, H_z^{(0)}(\bar{r};\bar{r}_s) + \iint\limits_{A_p+A_s} \nabla' \, G(\bar{r};\bar{r}') \times \bar{i}_o(\bar{r}')dx'dy' -$$

$$\iint\limits_{A_s} \nabla' \, G(\bar{r};\bar{r}') \times \bar{i}_o(\bar{r}')dx'dy' \qquad (2\text{-}31)$$

and letting

$$\bar{H}^{(p)}(\bar{r};\bar{r}_s) = \bar{a}_z H_z^{(0)}(\bar{r};\bar{r}_s) - \iint\limits_{A_p+A_s} \nabla' \, G(\bar{r};\bar{r}') \times \bar{i}_o(\bar{r}')dx'dy' \qquad (2\text{-}32)$$

we obtain

$$\bar{H}(\bar{r}) \simeq \bar{H}^{(p)}(\bar{r};\bar{r}_s) - \iint\limits_{A_s} \nabla' \, G(\bar{r};\bar{r}') \times \bar{i}_o(\bar{r}')dx'dy' \, . \qquad (2\text{-}33)$$

Notice that $\bar{H}^{(p)}(\bar{r};\bar{r}_s)$ is the magnetic field for the unslotted cylindrical plasma sheath. It is given explicitly in a scalar form in (B-14) for $r > c$, i.e., external to the plasma sheath.

For a wedge type slot we can carry out the integration in the φ-direction. For this purpose we write (2-33) in a scalar form

$$H_z(\bar{r}) \simeq H_z^{(p)}(\bar{r};\bar{r}_s) + H_z^{(s)}(\bar{r};\bar{r}_s) \qquad (2\text{-}34)$$

13

where

$$H_z^{(s)}(\bar{r};\bar{r}_s)\bar{a}_z = -\iint_{A_s} \nabla' G(\bar{r};\bar{r}') \times \bar{I}_o(\bar{r}')dx'dy' \qquad (2\text{-}35)$$

For the far-zone, we obtain from (B-14) that

$$H_z^{(p)}(\bar{r};\bar{r}_s) \sim \frac{j\omega\epsilon_o k'V}{(\pi k_o)^2 ab}\sqrt{\frac{2}{\pi k_o r}}\, e^{-j(k_o r - \pi/4)} \sum_{m=0}^{\infty} c_m j^m \frac{Q_m}{\Delta_m} \cos m(\varphi - \varphi_s) \qquad (2\text{-}36)$$

and from (2-35) that for a wedge slot of width $2\varphi_o$

$$H_z^{(s)}(\bar{r};\bar{r}_s) \sim \frac{\varphi_o}{4}\sqrt{\frac{2}{\pi k_o r}}\, e^{-j(k_o r - \pi/4)} \left\{ \frac{j\sigma k\epsilon_o V}{\pi^2 k_o \epsilon} \sum_{m=0}^{\infty}\sum_{n=0}^{\infty} j^n c_n c_m R_{nm}^{(2)} \Phi_{nm}^{(2)}(\varphi,\varphi_s) \right.$$

$$\left. + \frac{4\sigma\epsilon_o V}{\pi^2 k_o^2 \epsilon\, ab} \sum_{m=1}^{\infty}\sum_{n=1}^{\infty} nm j^n R_{nm}^{(1)} \Phi_{nm}^{(1)}(\varphi,\varphi_s) \right\} \qquad (2\text{-}37)$$

where

$$R_{nm}^{(2)} = (ab\,\Delta_m)^{-1}\int_b^c [N_m J_m'(kr) - M_m N_m'(kr)]\left[J_n'(k_o r) - \frac{J_n'(k_o a)}{H_n^{(2)'}(k_o a)} H_n^{(2)'}(k_o r) \right] r\,dr, \qquad (2\text{-}38)$$

$$R_{nm}^{(1)} = \Delta_m^{-1}\int_b^c [N_m J_m(kr) - M_m N_m(kr)]\left[-J_n(k_o r) + \frac{J_n'(k_o a)}{H_n^{(2)'}(k_o a)} H_n^{(2)}(k_o r) \right]\frac{dr}{r}, \qquad (2\text{-}39)$$

14

$$\Phi_{nm}^{(2)}(\varphi, \varphi_s) = \left[\frac{\sin(m-n)\varphi_0}{(m-n)\varphi_0}\right] \cos(n\varphi - m\varphi_s) + \left[\frac{\sin(m+n)\varphi_0}{(m+n)\varphi_0}\right] \cos(n\varphi + m\varphi_s),$$

$$(2\text{-}40)$$

$$\Phi_{nm}^{(1)}(\varphi, \varphi_s) = \left[\frac{\sin(m-n)\varphi_0}{(m-n)\varphi_0}\right] \sin(n\varphi - m\varphi_s) - \left[\frac{\sin(m+n)\varphi_0}{(m+n)\varphi_0}\right] \sin(n\varphi + m\varphi_s).$$

$$(2\text{-}41)$$

In (2-37) the first term arises from a circumferential current in the plasma slot, and the second term from a radial current. As $\varphi_0 \to 0$ we clearly see that $H_z^{(s)}(\bar{r}; \bar{r}_s) \to 0$. In the plasma slot we are assuming zero electron density, however, and hence the total electron current must be zero. The plasma slot current in (2-35) is the negative of the plasma sheath current without a slot, and thus when added to the latter produces zero electron current in the slot.

In other words, the first term on the right-hand-side of (2-34) is the magnetic field when the cylinder is enclosed by a continuous cylindrical plasma sheath. We can imagine that in the area where we want to create a slot we reduce the electron current to zero by adding there a current negative to that of the continuous plasma sheath. This current in the presence of a perfectly conducting cylinder gives rise to the second term on the right-hand-side of (2-34). This term acts as a source on the slotted plasma sheath and produces a new current there which has to be found in order to find $H_z(\bar{r})$ exactly. However, this leads to an integral equation that is not expected simpler in form than the basic one in (2-28).

The approximation (2-29) and (2-30) for the plasma current are expected to hold for underdense plasma $(\omega > \omega_p)$. For overdense plasma

15

$(\omega < \omega_p)$ the approximations may be appropriate only for slightly overdense case and large collision frequency. Because $G(\overline{r};\overline{r}')$ is the Green's function for the cylinder in the free space the representation (2-21) insures that for any approximate plasma current the fields automatically satisfy the boundary conditions at the cylinder and at infinity. However, only for the proper plasma current will the fields satisfy the boundary condition at the plasma sheath surface as well.

No doubt one may propose other approximations for the plasma current and carry out a series of calculations to study the effects of the underdense plasma sheath of various configurations on the cylindrical antenna. Lack of time prevents us to pursue these ideas for the present.

III

WAVEGUIDE APPROACH

3.1 Introduction

When the plasma sheath enclosing the antenna is of a substantial thickness it is well known that for the signal frequency ω sufficiently less than the plasma frequency ω_p negligible amount of power leaks through the sheath. Under these conditions if one opens a slot in the plasma sheath then it appears that the slot will act as a waveguide in transporting the power from the source to the outside free space. The waveguide transports the power via the propagating modes, if any exist. If only non-propagating modes exist, then the power transfer is very minimal because the fields attenuate exponentially in the guide. The plasma waveguide concept is of any use only when the electrical current does not penetrate the plasma sheath very much. This condition is satisfied where ω_p is sufficiently larger than ω. For this condition the integral equation approach to the problem becomes too unwieldy.

In the first part of this chapter we derive the tranverse magnetic modes in an infinite parallel plane plasma waveguide. The waveguide is formed by an infinite uniform plasma slab of plasma frequency sufficiently below ω while in the rest of the space the plasma frequency is sufficiently above ω. The mode derivation is elementary, except for finding the eigenvalues which is essentially a numerical job, except for some special cases when good approximate solutions are obtainable.

17

In the second part of the chapter, as an example, we consider a magnetic line source excited perfectly conducting cylinder enclosed by a closely fitting plasma sheath. We assume that a parallel face plasma slot is centered directly above the source and forms a parallel plate plasma waveguide. We select the waveguide width and the plasma parameters such as to make only the lower TM mode propagating. We compute the amplitude of the mode, and assuming the mode radiates without appreciable reflection at the external waveguide aperture, we are able to predict the magnetic line source excited perfectly conducting cylinder radiation through axially slotted plasma sheath of a particular configuration.

3.2 Transverse Magnetic Modes in a Parallel Plane Plasma Waveguide.

The waveguide is formed by two semi-infinite plasma slabs of uniform density separated a distance 2d and the gap filled by a lower density plasma. We introduce a cartesian coordinate system (x, y, z) with the y-axis normal to the plasma slabs and the origin at the half way point between them, as shown in Figure 3.1. The electrical conductivity of the plasma for, $|y| > d$,

$$\sigma = \frac{\epsilon_o \omega_{p1}^2}{\nu + j\omega} ,$$

(3-1)

and for $-d < y < d$,

$$\sigma = \frac{\epsilon_o \omega_{p1}^2}{\nu_1 + j\omega}$$

(3-2)

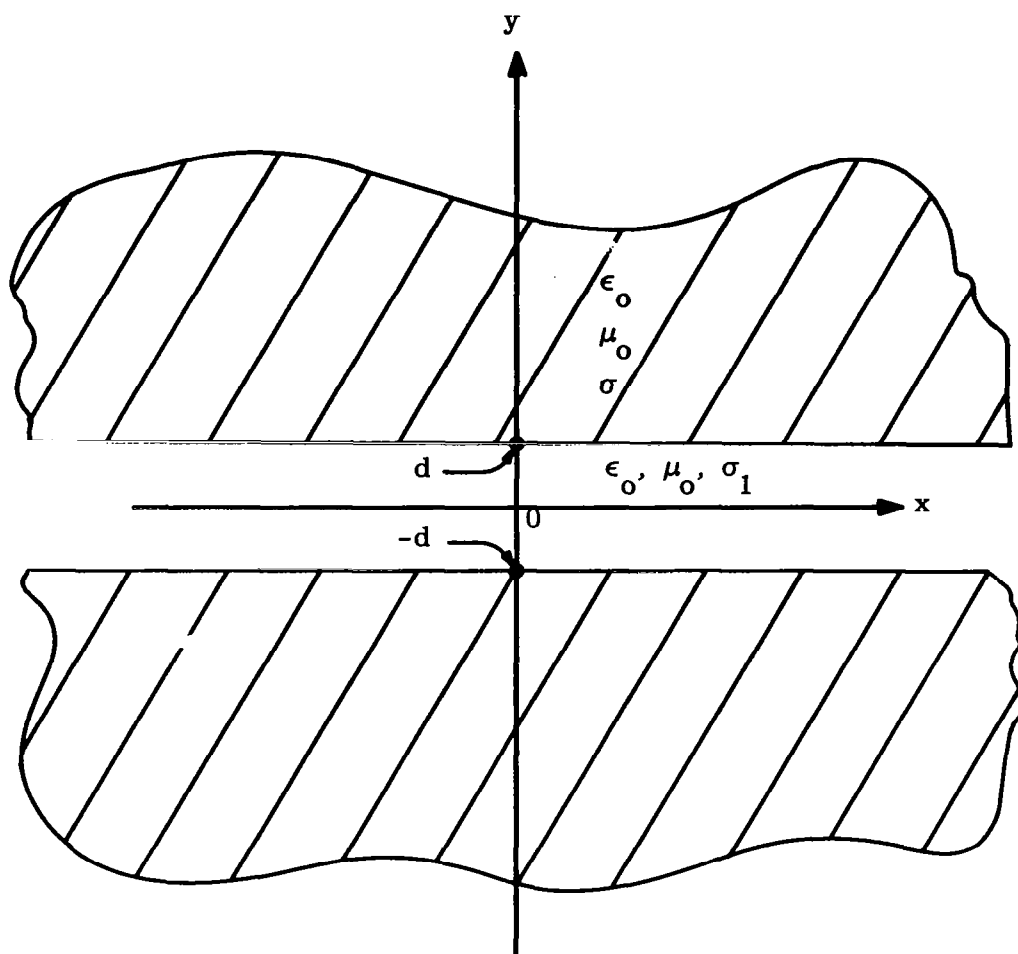where ω_p and ω_{p1} denote the plasma frequencies; ν and ν_1 the collision fre-

18

FIG. 3.1: PARALLEL PLANE PLASMA WAVEGUIDE (z = 0 cross section).

quencies, ω the signal frequency, and ϵ_o the free space permittivity. Taking the free space permeability μ_o completes the statement on the electromagnetic parameters of the problem.

The TM-modes in the parallel plane plasma waveguide have the following non-zero field components for propagation along the x-axis: $H_z(x,y)$, $E_x(x,y)$, $E_y(x,y)$, the $e^{j\omega t}$ time dependence being understood. Assuming that the fields have $\exp(-\gamma x)$ dependence in x, we obtain from the Maxwell's equations

$$H_z(x,y) = -\frac{j\omega\epsilon}{\gamma^2 + \omega^2\mu_o\epsilon} \frac{\partial}{\partial y} E_x(x,y) \qquad (3\text{-}3)$$

and

$$E_y(x,y) = -\frac{\gamma}{\gamma^2 + \omega^2\mu_o\epsilon} \frac{\partial}{\partial y} E_x(x,y) \qquad (3\text{-}4)$$

where

$$\epsilon = \epsilon_o - j\frac{\sigma}{\omega} .$$

Since all the field components satisfy the scalar wave equation, we have

$$E_x(x,y) = A \left\{ \begin{matrix} + \\ + \end{matrix} \right\} \exp(-Ky - \gamma x), \quad y > d, \qquad (3\text{-}5)$$

$$= B \left\{ \begin{matrix} \sin(K_1 y) \\ \cos(K_1 y) \end{matrix} \right\} \exp(-\gamma x), \quad -d < y < d, \qquad (3\text{-}6)$$

$$= A \left\{ \begin{matrix} - \\ + \end{matrix} \right\} \exp(Ky - \gamma x), \quad y < -d. \qquad (3\text{-}7)$$

and

$$\gamma^2 + k_1^2 = K_1^2 \qquad (3\text{-}8)$$

$$\gamma^2 + k^2 = -K^2 \qquad (3\text{-}9)$$

where $k = \omega\sqrt{\mu_0(\epsilon_0 - j\sigma/\omega)}$, $k_1 = \omega\sqrt{\mu_0(\epsilon_0 - j\sigma_1/\omega)}$, and the top line in the brackets refer to the symmetric mode, and the bottom line to the anti-symmetric mode. From (3-3) to (3-7) and the boundary conditions at $y = \pm d$ we obtain

$$\epsilon K_1 A + \begin{Bmatrix} -\cos(K_1 d) \\ +\sin(K_1 d) \end{Bmatrix} \epsilon_1 K \exp(Kd) B = 0 \qquad (3\text{-}10a)$$

$$A + \begin{Bmatrix} -\sin(K_1 d) \\ -\cos(K_1 d) \end{Bmatrix} \exp(Kd) B = 0. \qquad (3\text{-}10b)$$

The non-trivial solution of (3-10) exists only when the determinant of the coefficients vanishes, i.e.,

$$\frac{\epsilon_1 K}{\epsilon K_1} = \tan(K_1 d) , \qquad (3\text{-}11)$$

for the symmetric modes, and

$$\frac{\epsilon_1 K}{\epsilon K_1} = -\cot(K_1 d) \qquad (3\text{-}12)$$

for the anti-symmetric modes. Eliminating γ from (3-8) to (3-9) we obtain

$$K = \left[jk_o^2 \frac{\sigma - \sigma_1}{\omega\epsilon_o} - K_1^2 \right]^{1/2} \tag{3-13}$$

where $k_o = \omega\sqrt{\mu_o \epsilon_o}$ and thus from (3-11) and (3-12) we derive, respectively,

$$\frac{\omega\epsilon_o - j\sigma_1}{\omega\epsilon_o - j\sigma} \left[\frac{j(\sigma - \sigma_1)}{\omega\epsilon_o} \left(\frac{k_o}{K_1}\right)^2 - 1 \right]^{1/2} = \tan(K_1 d), \tag{3-14}$$

$$= -\cot(K_1 d). \tag{3-15}$$

Introducing dimensionless parameters

$$u = K_1 d \tag{3-16}$$

$$h = \frac{k_o d}{\pi} \; ; \; \left(h = \frac{2d}{\lambda_o} \; ; \; \lambda_o = \frac{2\pi}{k_o} \right) \tag{3-17}$$

$$X = \omega_p/\omega; \quad Y = \nu/\omega \tag{3-18}$$

$$X_1 = \omega_{p1}/\omega; \quad Y_1 = \nu_1/\omega \tag{3-19}$$

in the last two equations one obtains

$$\frac{1-jY}{1-jY_1} \; \frac{1-X_1^2 - jY_1}{1-X^2 - jY} \left\{ \left(\frac{\pi h}{u}\right)^2 \left[\frac{X^2}{1-jY} - \frac{X_1^2}{1-jY_1} \right] - 1 \right\}^{1/2}$$

$$= \tan u, \tag{3-20}$$

$$= -\cot u. \tag{3-21}$$

The appropriate roots u_0, u_2, u_4, ... of (3-20) and u_1, u_3, u_5, ... of (3-21) determine from (3-16) the eigenvalues

$$K_{ln} = \frac{u_n}{d} \, . \qquad \qquad \cdot \qquad \qquad (3\text{-}22)$$

The corresponding K_n and γ_n we compute by substituting (3-22) in (3-13) and (3-8). Thus one has to solve first for the roots of (3-20) and (3-21) before it is possible to exhibit explicitly the various TM modes in the parallel plane plasma waveguide.

The Loss-Less Case: $Y = Y_1 = 0$. The task of finding the roots of (3-20) and (3-21) is largely a numerical one. Primarily for this reason we restrict the calculation to the loss-less case. This permits us to exhibit the main features of the plasma waveguide with a minimum of numerical work. The results would be only trivialy modified for a slightly lossy plasma guide, except for some special cases.

For the loss-less case (3-20) and (3-21) become, respectively,

$$-\left(\frac{1-x_1^2}{x^2-1}\right)\left[\left(\frac{\pi h}{u}\right)^2\left(x^2 - x_1^2\right) - 1\right]^{1/2} = \tan u, \qquad (3\text{-}23)$$

$$= -\cot u. \qquad (3\text{-}24)$$

The plasma waveguide exists in any meaningful fashion only when

23

$$0 \leq X_1 < 1; \quad X > 1, \tag{3-25}$$

and hence in the subsequent discussion we implicitly require these inequalities to be satisfied. Further, a particular mode n for a given h, X, X_1 will exist only if u_n exists. In the loss-less case u_n is real and it can exist only when

$$h \left[X^2 - X_1^2 \right]^{1/2} > \frac{n}{2} \tag{3-26}$$

as can be deduced from (3-23) and (3-24). The equation

$$h \left[X^2 - X_1^2 \right]^{1/2} = \frac{n}{2} \tag{3-27}$$

defines a boundary in the X-h plane that separates the regions of existence and non-existence for the TM_n mode. We note that the zeroth order mode exists for any h, the plasma parameters X and X_1 being only subject to (3-25).

Before we introduce the numerical results it is instructive to present the roots u_n for some special cases. From (3-23) we obtain for the zeroth order mode

$$u_0 \simeq - \frac{1-X_1^2}{\pi h X}, \quad X \gg 1, \tag{3-28a}$$

$$u_0 \to -\pi h \sqrt{1-X_1^2}, \quad X \to 1, \quad h < \frac{1}{2\sqrt{1-X_1^2}}, \tag{3-28b}$$

$$u_o \to -\frac{\pi}{2} \; , \quad X \to 1 \; , \quad h > \frac{1}{2\sqrt{1-X_1^2}} \; . \tag{3-28c}$$

From (3-23) and (3-24), whenever (3-26) is satisfied, we obtain for the higher order modes

$$u_n \simeq \frac{\pi n}{2} - \frac{h}{X}(1 - X_1^2) \; , \quad X >> 1 \; , \tag{3-29a}$$

$$u_n \to \frac{\pi}{2}(n - 1) \; , \quad X \to 1 \; , \tag{3-29b}$$

with $n = 1, 3, 5, \ldots$ for the anti-symmetric modes, and $n = 2, 4, 6, \ldots$ for the symmetric modes. It is evident that u_o is of the lowest order mode, u_1 of the next higher order mode, etc. Furthermore, as expected, when $X \to \infty$ the roots reduce to those of the perfectly conducting parallel plane guide. The lower order mode, TM_o, then propagates for any guide width. At times we shall refer to TM_o as the principal mode.

The lowest order mode is of the most practical importance. We present in Figure 3.2 u_o as a function of X for the guide width $h = 1.0$, 0.75, 0.50, and 0.25 fractions of the free space wavelength, and $X_1 = 0$ and 0.75. We note that increasing the normalized plasma frequency X_1 in the guide decreases the magnitude of u_o. However, this does not mean that the cut-off frequency will decrease. We shall see shortly, in fact, that the opposite is true.

The constant K which determines the rate of the field attenuation in the semi-infinite plasma slabs we compute from (3-13) for the loss-less case as
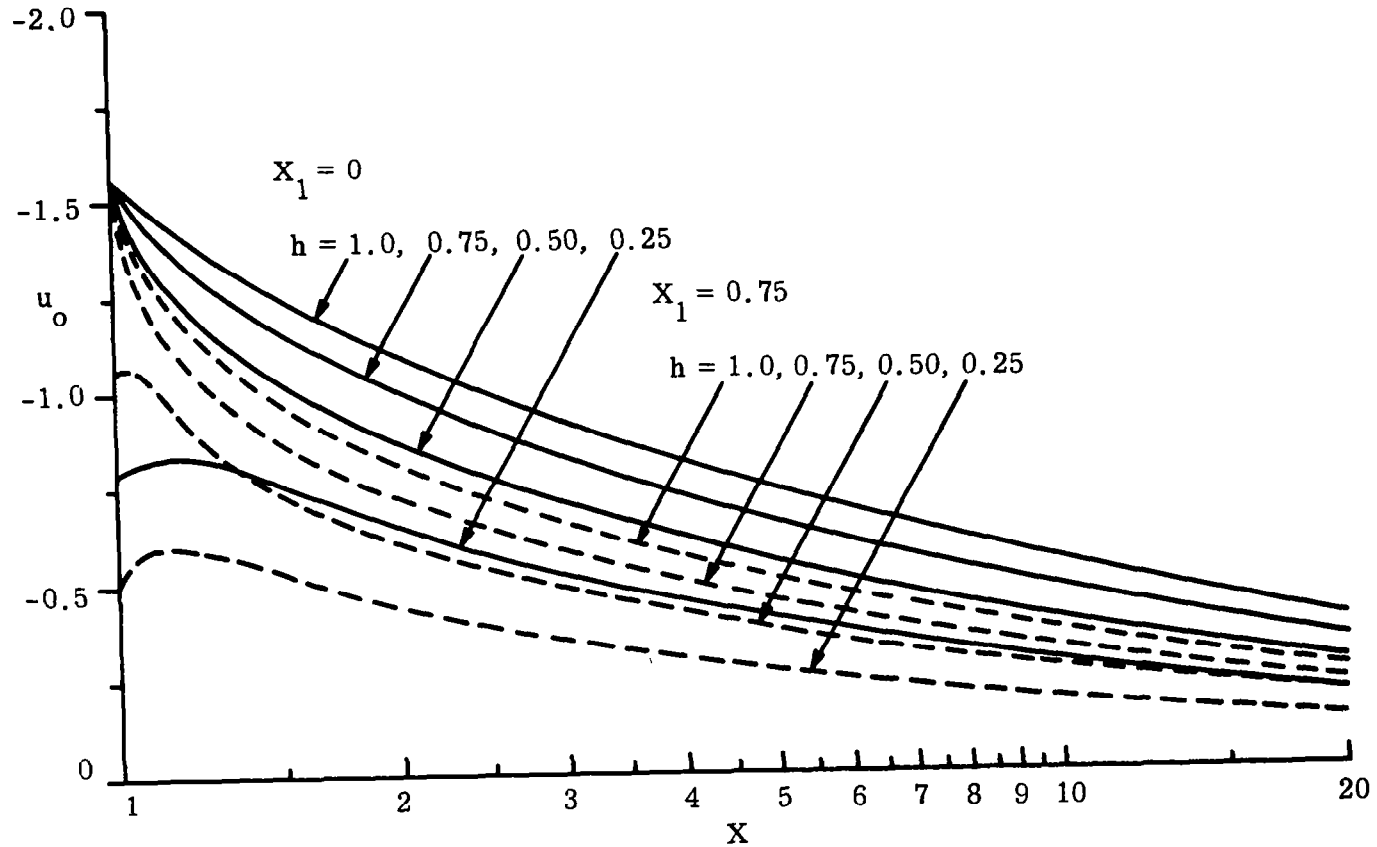
25

FIG. 3.2: THE LOWEST ORDER ROOT u_o OF (3-23) FOR THE PARALLEL PLANE PLASMA WAVEGUIDE AS A FUNCTION OF X WITH X_1 AND h AS A PARAMETER, AND $Y = Y_1 = 0$.

$$K_n = k_o \left[x^2 - x_1^2 - \left(\frac{u_n}{\pi h} \right)^2 \right]^{1/2} . \qquad (3\text{-}30)$$

We find from (3-8) the propagation constant

$$\gamma_n = k_o \left[\left(\frac{u_n}{\pi h} \right)^2 + x_1^2 - 1 \right]^{1/2} . \qquad (3\text{-}31)$$

We define

$$\gamma_n = \alpha_n + j\beta_n \qquad (3\text{-}32)$$

where α_n is the attenuation constant, and β_n is the phase constant; both constants are real and positive. The TM_n mode is propagating in a loss-less guide when

$$\alpha_n = 0 \ , \quad \beta_n = k_o \left[1 - \left(\frac{u_n}{\pi h} \right)^2 - x_1^2 \right]^{1/2} , \qquad (3\text{-}33)$$

with

$$\left(\frac{u_n}{\pi h} \right)^2 + x_1^2 < 1 \ , \qquad (3\text{-}34)$$

and beyond cut-off when

$$\alpha_n = k_o \left[\frac{u_n^2}{(\pi h)^2} + x_1^2 - 1 \right]^{1/2} ; \quad \beta_n = 0 \ , \qquad (3\text{-}35)$$

with

$$\frac{u_n^2}{(\pi h)^2} + X_1^2 > 1 , \qquad\qquad (3\text{-}36)$$

as can be shown from (3-31). Since $u_n = u_n(h, X, X_1)$ we see from (3-34) and (3-36) that the equation, when it exists,

$$u_n^2(h, X, X_1) = (\pi h)^2(1 - X_1^2) \qquad\qquad (3\text{-}37)$$

defines a curve in the X-h plane that separates the propagation region from the non-propagation one. In Fig. 3.3 we show these curves for $X_1 = 0$, 0.75, and 0.90 in the cases of TM_o and TM_2 modes. We have left out of the discussion TM_1 mode because in the particular configuration we consider at the end of this chapter, it is not excited by the source. The solid curves refer to the TM_o mode, and the dashed curves to TM_2 mode. The area bounded by the coordinate axis and the solid curve is the region of beyond cutoff for the TM_o mode, the rest of the quadrant being the region of propagation. We notice that the cutoff region increases only very slightly as X_1 increases from 0 to 0.9. However, when $X_1 \rightarrow 1$, the TM_o mode is beyond cutoff for any h and X.

The coordinate axis and the curve

$$h[X^2 - X_1^2]^{1/2} = 1 \qquad\qquad (3\text{-}38)$$

bound the region of non-existence of the TM_2 mode. We have not plotted this curve in Fig. 3.3 because it would make the figure too crowded, and furthermore for our discussion later on this curve is not important. The
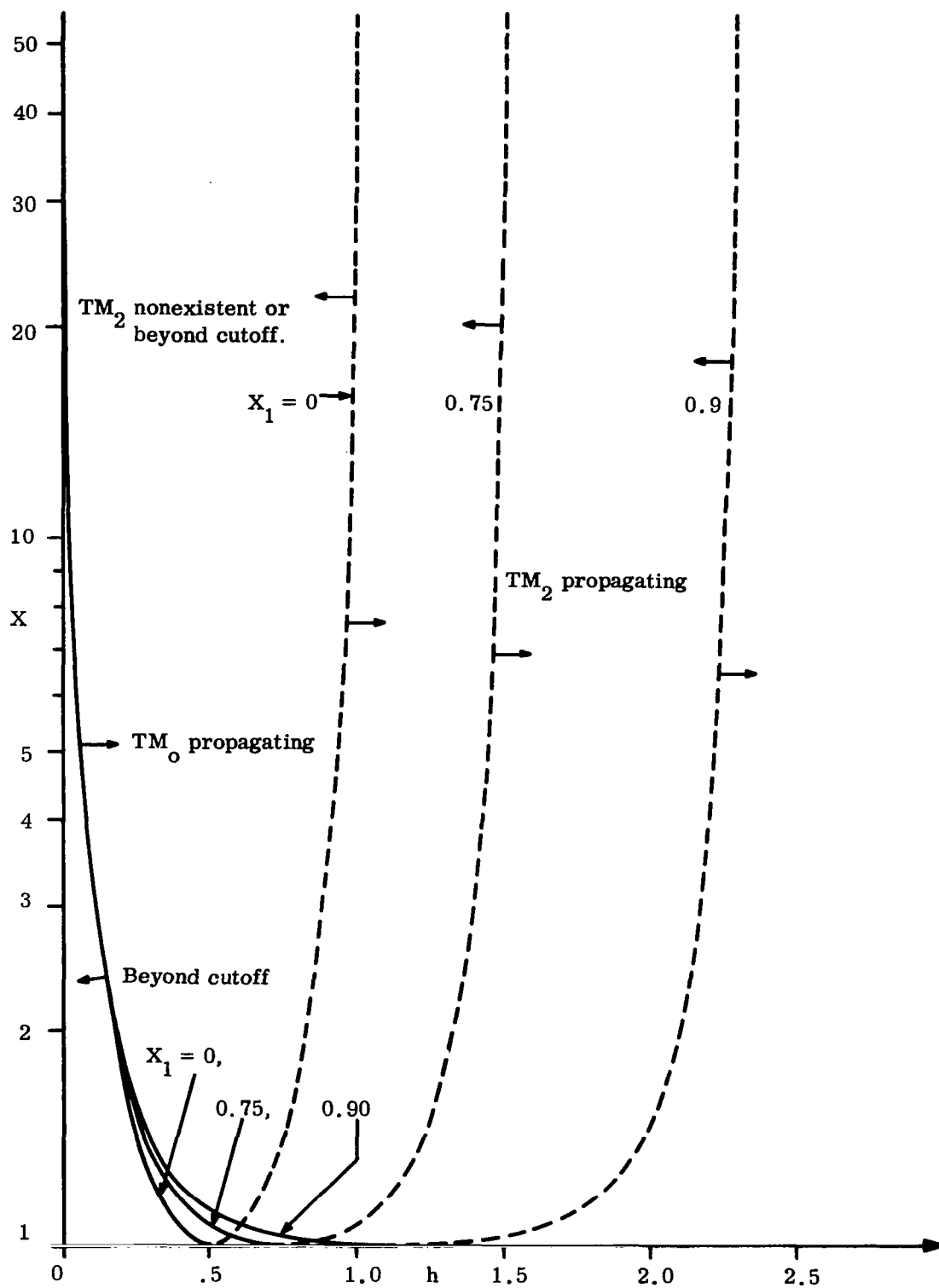
28

FIG. 3.3: THE REGIONS OF PROPAGATION, BEYOND CUTOFF, AND NONEXISTENCE FOR TM_o AND TM_2 MODES.

29

area between the curve (3-38) and those shown dashed in Fig. 3.3 is the beyond-cutoff region. The area to the right of the dashed curve is the propagation region. As X_1 increases from 0 to 1-0 the dashed curve moves to the right in noticeable steps, i.e., the region of propagating becomes significantly reduced. In fact, we may easily predict the propagation - beyond cutoff boundary as a function of X_1 from (3-29a), and (3-37) for any mode, other than the zeroth, when $X \gg 1$, i.e.,

$$h = \frac{n}{2\sqrt{1 - X_1^2}} \quad , \quad n \neq 0. \tag{3-39}$$

The Modal Fields. Letting $B \to K_{1n}B_n$ we obtain from (3-3) to (3-12) TM_n mode fields

$$E_x^{(n)}(x,y) = B_n K_{1n} \begin{Bmatrix} \sin(K_{1n}d) \\ \cos(K_{1n}d) \end{Bmatrix} e^{-[K_n(y-d)+\gamma_n x]} \quad , \quad y > d , \quad \begin{matrix} (3\text{-}40a) \\ (3\text{-}40b) \end{matrix}$$

$$= B_n K_{1n} \begin{Bmatrix} \sin(K_{1n}y) \\ \cos(K_{1n}y) \end{Bmatrix} e^{-\gamma_n x} \quad , \qquad -d < y < d, \quad \begin{matrix} (3\text{-}41a) \\ (3\text{-}41b) \end{matrix}$$

$$= B_n K_{1n} \begin{Bmatrix} -\sin(K_{1n}d) \\ \cos(K_{1n}d) \end{Bmatrix} e^{-[K_n(-y-d)+\gamma_n x]} \quad , \quad y < -d , \quad \begin{matrix} (3\text{-}42a) \\ (3\text{-}42b) \end{matrix}$$

$$H_z^{(n)}(x,y) = B_n j\omega\epsilon_1 \begin{Bmatrix} -\cos(K_{1n}d) \\ \sin(K_{1n}d) \end{Bmatrix} e^{-[K_n(y-d)+\gamma_n x]}, \quad y > d , \quad \begin{matrix} (3\text{-}43a) \\ (3\text{-}43b) \end{matrix}$$

$$= B_n j\omega\epsilon_1 \begin{Bmatrix} -\cos(K_{1n}y) \\ \sin(K_{1n}y) \end{Bmatrix} e^{-\gamma_n x} \quad , \qquad -d < y < d, \quad \begin{matrix} (3\text{-}44a) \\ (3\text{-}44b) \end{matrix}$$

30

$$= B_n j \omega \epsilon_1 \begin{Bmatrix} -\cos(K_{1n}d) \\ -\sin(K_{1n}d) \end{Bmatrix} e^{-[K_n(-y-d)+\gamma_n x]} \qquad \begin{matrix} (3\text{-}45\text{a}) \\ , \; y < -d. \quad (3\text{-}45\text{b}) \end{matrix}$$

The top line, in the brackets, as before, refers to the symmetric mode $(n=0,2,4,\cdots)$, and the bottom line to the anti-symmetric mode $(n=1,3,5,\ldots)$. The electric field component $E_y(x,y)$ can be computed for either symmetry from

$$E_y^{(n)}(x,y) = \frac{\gamma_n}{j\omega\epsilon} H_z^{(n)}(x,y) \;, \qquad |y| > d \qquad (3\text{-}46)$$

$$= \frac{\gamma_n}{j\omega\epsilon_1} H_z^{(n)}(x,y), \quad -d < y < d. \qquad (3\text{-}47)$$

This completes the discussion of the TM modes in the parallel plate plasma waveguide. The zeroth order mode from this set is used in the calculation of the radiation by a slot in a plasma sheath.

3.3 Application of the Principal Mode to the Slotted Sheath Problem.

As an example of the application of the principal mode to the slotted sheath problem we consider the configuration shown in Fig. 3.4. A magnetic line source excited perfectly conducting cylinder of radius a in free space is enclosed by a plasma sheath of radius c. The plasma sheath is in a contact with the cylinder. The plasma sheath has uniform conductivity σ, except for the parallel plate plasma waveguide where the conductivity is σ_1. The plasma waveguide is centered with respect to the magnetic line source. The free space permittivity ϵ_o and the free space permeability μ_o complete the specification of the electromagnetic parameters of the plasma sheath.

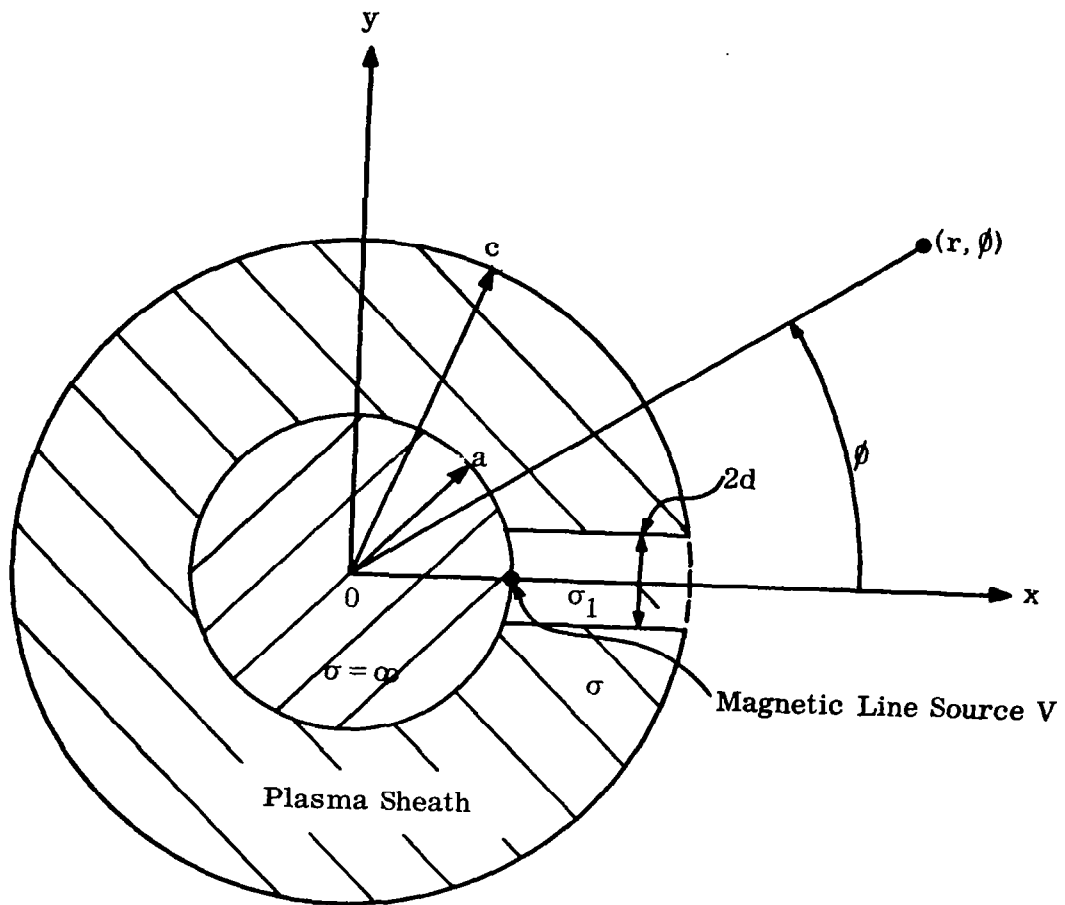First we obtain an external field representation $(r > c)$ in terms of the

FIG. 3.4: CONFIGURATION OF A PLASMA SLOT PROBLEM.

tangential electric field at $r = c$. The latter we approximate by the plasma waveguide aperture field derived from the principal mode calculations. The first part of this analysis is exact, the second part is approximate.

From (2-15) and (2-18) we may show that

$$H_z(r,\varphi) = j\omega\epsilon_o c \int_{-\pi}^{\pi} G(r,\varphi;c,\varphi') \bar{E}(c,\varphi') \cdot \bar{a}_{\varphi'} d\varphi' \qquad (3\text{-}48)$$

For $r > c$ we find from (2-17) that assuming $a \rightarrow c$

$$G(r,\varphi;c,\varphi') = \frac{1}{2\pi k_o c} \sum_{n=0}^{\infty} c_n \frac{H_n^{(2)}(k_o r)}{H_n^{(2)'}(k_o c)} \cos n(\varphi-\varphi'). \qquad (3\text{-}49)$$

Let

$$\bar{E}(c,\varphi') \cdot \bar{a}_{\varphi'} = E_o f(\varphi') \qquad (3\text{-}50)$$

where E_o is a constant, then in the far-zone $(r \gg c)$

$$H_z(r,\varphi) = -j \frac{1}{2\pi} \sqrt{\frac{\epsilon_o}{\mu_o}} E_o \sqrt{\frac{2}{\pi k_o r}} e^{-j(k_o r - \pi/4)} F(\varphi), \qquad (3\text{-}51)$$

with

$$F(\varphi) = \sum_{n=0}^{\infty} \left[\frac{c_n j^n}{H_n^{(2)'}(k_o c)} \int_{-\pi}^{\pi} f(\varphi') \cos n(\varphi-\varphi') d\varphi' \right]. \qquad (3\text{-}52)$$

We define the gain function of the plasma sheath slot by

$$G_o(\varphi) = \frac{|F(\varphi)|^2}{\frac{1}{2\pi} \int_{-\pi}^{\pi} |F(\varphi)|^2 d\varphi} \qquad (3\text{-}53)$$

33

The plasma waveguide radiation we normalize with respect to the forward radiation in the free space of the magnetic line source excited cylinder, i.e.,

$$W(\varphi) \equiv \frac{\left| H_z(r,\varphi) \text{ of } (3\text{-}51) \right|^2}{\left| H_z(r,0) \text{ of } (A\text{-}8) \right|^2} \quad , \quad r \gg a \; .$$

(3-54)

It is easy to reduce (3-54) to the form

$$W(\varphi) = \frac{P \, G_o(\varphi)}{P(0)} \quad , $$

(3-55)

where the power radiated through the plasma sheath, per unit length of the cylinder,

$$P = \frac{1}{2}\sqrt{\frac{\mu_o}{\epsilon_o}} \int_0^{2\pi} \left| H_z(r,\varphi) \right|^2 r\,d\varphi \; , \quad r \gg c \; ,$$

(3-56)

and

$$P(0) = \frac{1}{2}\sqrt{\frac{\mu_o}{\epsilon_o}} \left| H_z(r,0) \text{ of } (A\text{-}8) \right|^2 2\pi r \; , \quad r \gg a \; .$$

(3-57)

The latter power is computed for an omnidirectional source whose radiation is of the same intensity as that of the forward radiation of the magnetic line source excited perfectly conducting cylinder in the free space.

The power flow (time average), per unit length, in the positive x-direction of the parallel face plasma waveguide for the TM_n mode is given by

$$P_n = \frac{1}{2} \, \text{Re} \int_{-\infty}^{\infty} E_y(x,y) \, H_z^*(x,y)\,dy \; .$$

(3-58)

34

For the loss-less case the power flow in the principal mode

$$P_o = \omega \epsilon_1 \beta_o |B_o|^2 \frac{d}{2} \left[1 + \frac{\text{Sin}(2u_o)}{2u_o} + \frac{\epsilon_1}{\epsilon} \frac{\text{Cos}^2(u_o)}{2K_1 d} \right] . \qquad (3\text{-}59)$$

When the guide is only slightly lossy then the form of (3-59) is multiplied bye $\exp[2\alpha_o(x-a)]$, where α_o is the attenuation constant. Assuming that the principal mode radiates from the plasma waveguide aperture without reflections we obtain

$$P = P_o e^{-2\alpha_o(c-a)} . \qquad (3\text{-}60)$$

For the calculation of the principal mode amplitude we refer to Fig. 3.5 which is a section of Fig. 3.4 in order to show some of the details. The coordinate origin also has been shifted to the right a distance a, as a matter of convenience for the calculation. The electric and magnetic fields produced by the magnetic line source satisfy

$$\oint_C \bar{E} \cdot d\bar{l} = -j\omega\mu_o \iint_A H_z dxdy - V . \qquad (3\text{-}61)$$

For our calculation we take the path C as shown in Fig. 3.5. The area A is enclosed by the path C. The electric field for $x > 0$ in the plasma slot may be represented by infinite series of terms (3-47). No such expansion is possible in area A which is bounded by the cylinder, the y-axis, and the guide walls. Thus we obtain from (3-61)
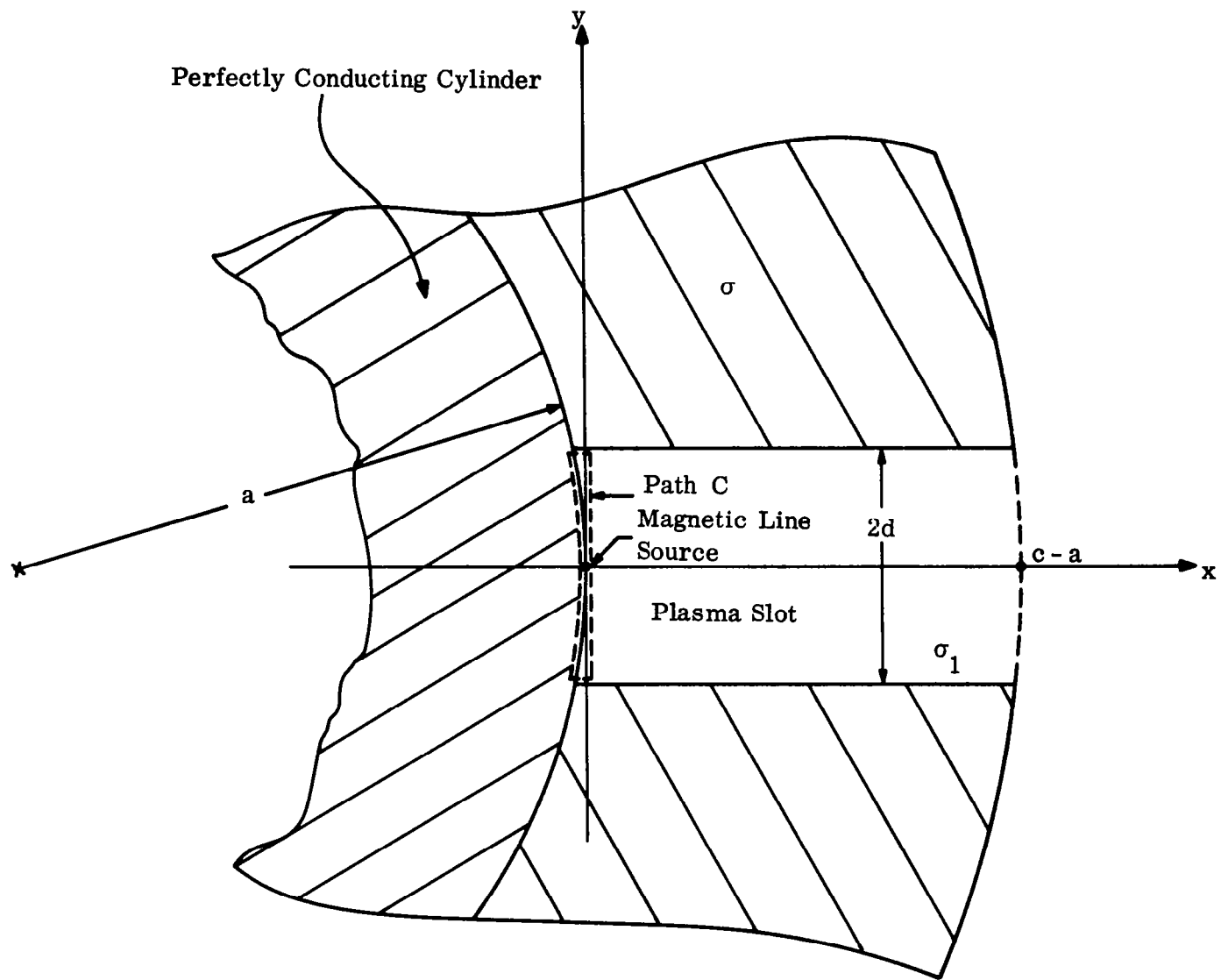
FIG. 3.5: CONFIGURATION FOR THE CALCULATION OF THE PRINCIPAL MODE
AMPLITUDE.

$$-\sum_{n,\,even} B_n \gamma_n \; 2d \; \frac{\mathrm{Sin}(u_n)}{(u_n)} \; + \; \int_0^{-x_o} [E_x(x,d)-E_x(x,-d)]dx \; =$$

$$-j\omega\mu_o \iint_A H_z(x,y)dxdy \; - \; V \qquad\qquad (3\text{-}62)$$

where $x_o = a - a \; \mathrm{Cos}[\text{arc } \sin \frac{d}{a}]$.

When the plasma sheath conductivity σ, and the cylinder radius a are sufficiently large we may neglect the two integrals, as well as all the terms in the series, except the zeroth term, i.e.,

$$B_o \simeq \frac{V}{\gamma_o 2d} \; \frac{(u_o)}{\mathrm{Sin}(u_o)} \; . \qquad\qquad (3\text{-}63)$$

This result becomes exact when $|\sigma| \rightarrow \infty$, $a \rightarrow \infty$.

The result (3-63) will not be altered when the magnetic line source is moved to any position on the cylinder surface, inside the guide walls. Only symmetric TM_n modes (n-even) will be excited when the source is in the symmetric position shown; anti-symmetric modes in addition will be excited when the source is moved off the x-axis.

From (3-47) and (3-50) we see that the plasma slot aperture field distribution

$$f(\varphi) \simeq \mathrm{Cos} \; (K_{10}c\varphi), \; \varphi \simeq y/c \quad . \qquad\qquad (3\text{-}64)$$

This approximate form should hold for the plasma slot width $h \lesssim 0.5$; certainly as far as the gain function calculation is concerned. For sufficiently large conductivity of the plasma sheath one may take $f(\varphi) \sim 0$ on the plasma sheath surface. Thus we find

$$\int_{-\pi}^{\pi} f(\varphi') \, \cos n(\varphi-\varphi') \, d\varphi' \simeq \int_{-\varphi_o}^{\varphi_o} \cos(K_{10}c\varphi') \, \cos n(\varphi-\varphi') d\varphi' =$$

$$\varphi_o a_n \, \cos n \, \varphi \qquad\qquad (3\text{-}65)$$

where

$$\varphi_o = \text{arc sin } (\pi \frac{h}{k_o c}) = \arcsin \left(\frac{d}{c}\right) , \qquad\qquad (3\text{-}66)$$

$$a_n = \frac{\sin(u_o'- n)\varphi_o}{(u_o' - n)\varphi_o} + \frac{\sin(u_o' + n)\varphi_o}{(u_o' + n)\varphi_o} , \qquad\qquad (3\text{-}67)$$

and $u_o' = \dfrac{u_o c}{d} = \dfrac{u_o}{\pi} \dfrac{k_o c}{h}$.

Substituting (3-65) in (3-52) and the resulting equation in (3-53) we obtain

$$G_o(\varphi) \simeq \frac{\left| \sum\limits_{n=0}^{\infty} c_n j^n \dfrac{a_n \cos(n\varphi)}{H_n^{(2)'}(k_o c)} \right|^2}{\sum\limits_{n=0}^{\infty} c_n \left| \dfrac{a_n}{H_n^{(2)'}(k_o c)} \right|^2} . \qquad\qquad (3\text{-}68)$$

We observe that the gain functions of the magnetic line source excited perfectly conducting cylinder is obtained from (3-68) by letting $a_n \rightarrow 1$, and $c \rightarrow a$. This result is exact.

For sufficiently high plasma conductivity σ one may neglect the third

term in (3-59) and then substituting (3-63) in (3-59) we obtain

$$P_o \simeq \frac{\omega \epsilon_1 \beta_o v^2}{8d(\alpha_o^2 + \beta_o^2)} \left(1 + \frac{\sin 2u_o}{2u_o}\right) \left(\frac{u_o}{\sin u_o}\right)^2 . \qquad (3\text{-}69)$$

From (3-57) we find

$$P(0) = \frac{v^2 \sqrt{\frac{\epsilon_o}{\mu_o}}}{2\pi^2 k_o a^2} \left| \sum_{n=0}^{\infty} \frac{c_n j^n}{H_n^{(2)'}(k_o a)} \right|^2 \qquad (3\text{-}70)$$

and hence

$$\frac{P_o}{P(0)} \simeq \frac{\pi (k_o a)^2 \beta_o k_o \epsilon_1}{4h(\alpha_o^2 + \beta_o^2) \epsilon_o} \frac{\left[1 + \frac{\sin 2u_o}{2u_o}\right] \left(\frac{u_o}{\sin u_o}\right)^2}{\left| \sum_{n=0}^{\infty} \frac{c_n j^n}{H_n^{(2)'}(k_o a)} \right|^2} . \qquad (3\text{-}71)$$

From (3-55) and (3-60) we have

$$W(\varphi) = \frac{P_o}{P(0)} e^{-2\alpha_o(c-a)} G_o(\varphi) . \qquad (3\text{-}72)$$

For loss-less plasma, as can be shown from (3-71), we may set the factor

$$\frac{P_o}{P(0)} \simeq \frac{\pi}{4} \frac{(k_o a)^2 (1 - X_1^2)}{h[1 - (\frac{u_o}{\pi h})^2 - X_1^2]^{1/2}} \frac{[1 + \frac{\sin 2u_o}{2u_o}] (\frac{u_o}{\sin u_o})^2}{\left| \sum_{n=0}^{\infty} \frac{c_n j^n}{H_n^{(2)'}(k_o a)} \right|^2} . \qquad (3\text{-}73)$$

39

In Fig. 3.6 we have plotted from (3-73) the normalized power coupled from the magnetic line source into the parallel plate plasma waveguide principal mode as a function of the normalized plasma frequency X. This power is the same as the power coupled into the waveguide, because only the principal mode is propagating for the parameter values under consideration, namely h = 0.25, 0.5; and X_1 = 0, 0.75, 0.9. The coupling curves are essentially flat for X > 4, and increasing for X > 4 as a consequence of u_0 increasing. When X → 1, the approximation of (3-73) becomes seriously questionable. Decreasing the guide width from h=0.5 to h=0.25 increases the power coupled into the guide approximately by a factor of two as can be seen from the graphs, and can also be verified by inspection of (3-73), assuming that u_0 did not change appreciably. Increasing the plasma frequency in the guide X_1, however, decreases the power coupled into the guide. In the limit of X_1 → 1 we would have zero power coupling. This behaviour becomes obvious also if we consider the characteristic impedance of the plasma waveguide for the principal mode. We may show that for large X the characteristic impedance

$$Z_0 = \frac{2\pi h}{k_0} \sqrt{\frac{\mu_0}{\epsilon_0}} \quad \frac{[1 - (\frac{u_0}{\pi h})^2 - X_1^2]^{1/2}}{(1 - X_1^2)} \tag{3-74}$$

and the power coupled into the guide of unit width is V^2/Z_0 (not normalized). The behaviour of the graphs in Fig. 3.6 then follows: decreasing h reduces Z_0 and hence increases the power coupling; increasing X_1 produces an increase in Z_0 and hence a decrease in power coupling. Further we have to add that according to (3-73) $P_0/P(0)$ is real when the TM_0 mode is propagating
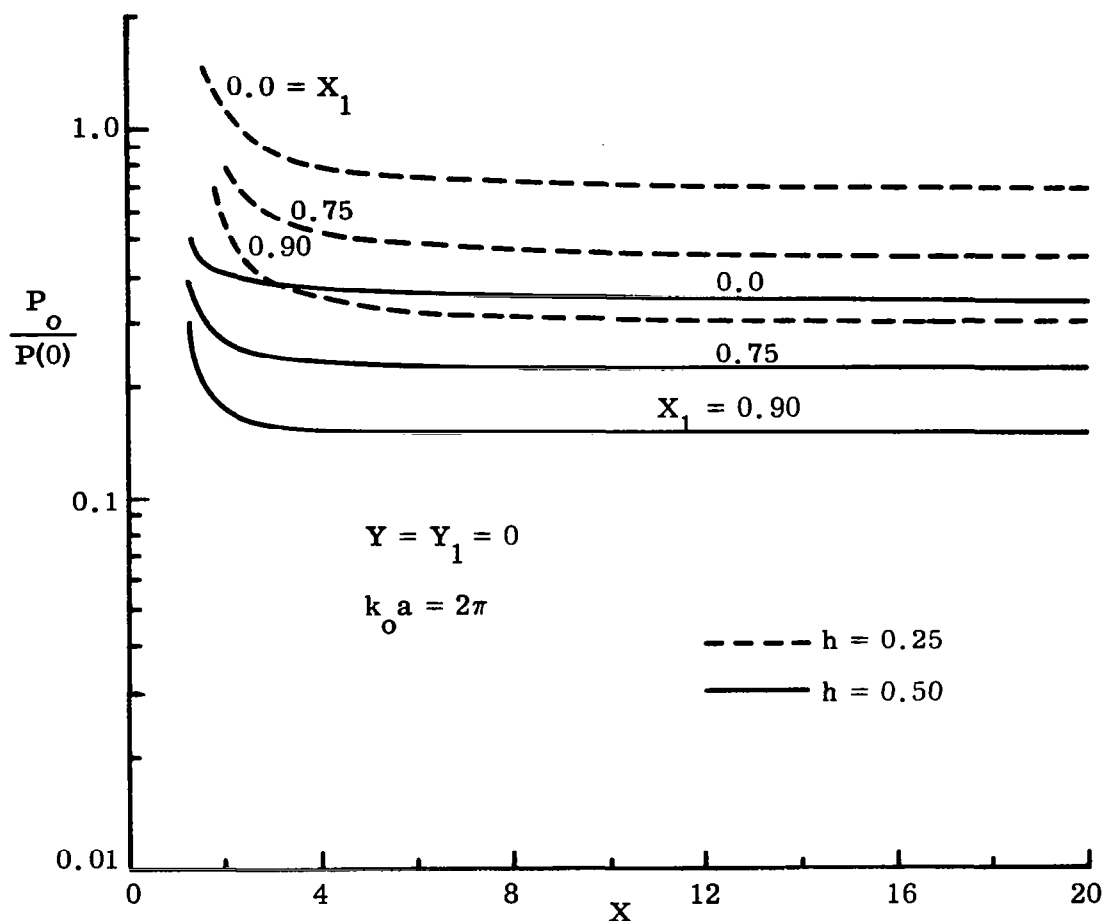
40

FIG. 3.6: POWER COUPLED (NORMALIZED) INTO THE PRINCIPAL MODE
OF THE WAVEGUIDE AS A FUNCTION OF X. THE PARAMETERS
ARE h AND X_1.

and imaginary when the mode is beyond-cutoff. At the cutoff we have spurious singularity.

Since the plasma is loss-less and in addition the parameters are such that the principal mode is propagating we have that $\alpha_o = 0$, and hence $\exp[2\alpha_o(c-b)] = 1$.

The last factor in (3-72) is the gain function $G_o(\varphi)$ of the axial slot excited cylinder of radius c. The axial slot is excited by the principal mode (TM_o-mode) of the parallel plate plasma waveguide. We show $G_o(\varphi)$ in Fig. 3.7 for the case of $k_o c = 4\pi$; $Y = Y_1 = X_1 = 0$; $X = 4$ and $h = 0.25$, and 0.50. The curves did not change for all practical purposes as X was increased to 20 and X_1 to 0.9. The $G_o(\varphi)$ calculated is symmetric with respect to $\varphi = 0$ and very broad and smooth in the forward direction, but with some lobing in the back. The smooth behaviour of the gain function for $-120° < \varphi < 120°$ results from the slot width being less than one half wavelength wide and the plasma sheath having insignificant leakage of power. A wider slot and hence a wider parallel plate plasma waveguide could support some higher order modes. For example the next mode above the principal one, TM_1, produces an anti-symmetric contribution to the aperture field and hence the gain function will no longer have a maximum in the forward direction, but off to one side, depending on the relative phasing of TM_1 to TM_o mode. The lobing in the back arises from the surface waves which travel around the cylinder. The gain function calculation should be accurate in the forward semi-circle; in the back semi-circle it should be accurate for large X. As X tends to approach unity the surface wave characteristics are apt to change and hence the lobing in the back will change.
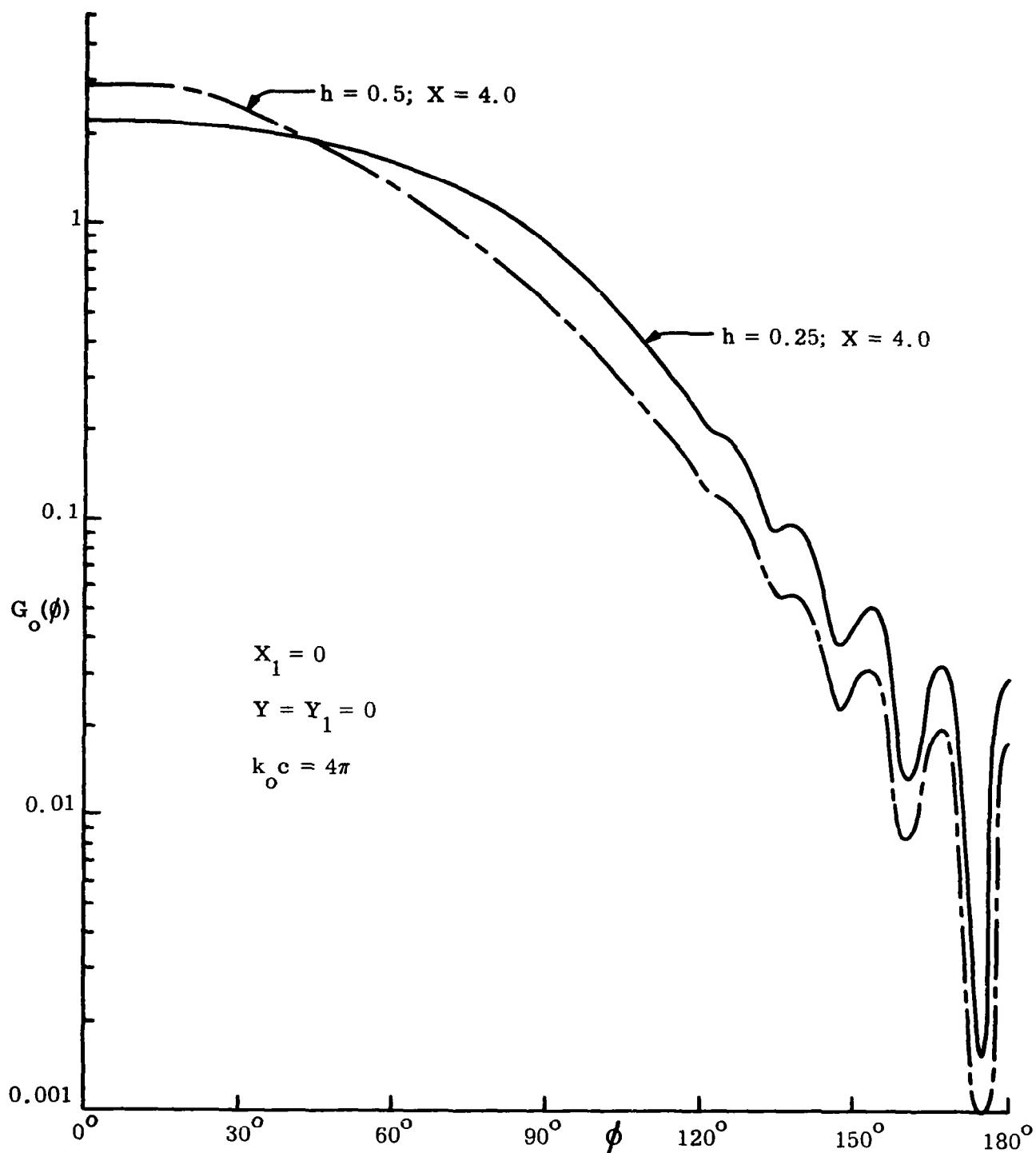
FIG. 3.7: GAIN FUNCTION OF TWO WAVELENGTH RADIUS CYLINDER WITH THE
SLOT WIDTH h A PARAMETER.

43

The radiation of the plasma slot normalized to the forward radiation of the cylinder antenna in the free space, $W(\varphi)$, are the products of $[G_o(\varphi)][P_o/P(0)]$, for the range of parameters considered. Thus in our case $W(\varphi)$ is simply a $G_o(\varphi)$ with a change in normalization. For this reason we consider $W(\varphi)$ for $\varphi=0$, i.e., $W(0)$. We plot $W(0)$ as a function of X in Fig. 3.8 with the same parameters as for the ratio $P_o/P(0)$. The $W(0)$ curves are essentially flat for $X > 4$ and tend to peak as $X \rightarrow 1$. These characteristics are due to the coupling coefficient $P_o/P(0)$. We observe that the radiation is re-established when the plasma guide width h=0.5 and $X_1 = 0$ (no plasma in the guide). As X_1 increases to 1.0 a moderate attenuation sets in, if X_1 would exceed 1.0 a very severe attenuation would result. Decreasing the guide width by one half actually increases the radiations by approximately 50%. This results from a more effective coupling of the line source to the waveguide. However, the resulting enhancement of the waveguide fields, if we narrow the waveguide width very much, may result in the break-down of the plasma and thus make this analysis inapplicable.

When the plasma sheath is shielded from the perfectly conducting cylinder by a dielectric layer, then the analysis to find the power coupled into the plasma waveguide becomes considerably more involved. Particularly so when the source is not facing the plasma slot. For the plasma density sufficiently large so that no direct radiation through the sheath is possible, an annular waveguide is formed by the dielectric between the cylinder and the sheath. The fields in the annular waveguide are composed of an infinite set of standing waves, and at some angular positions deep minimas will result.
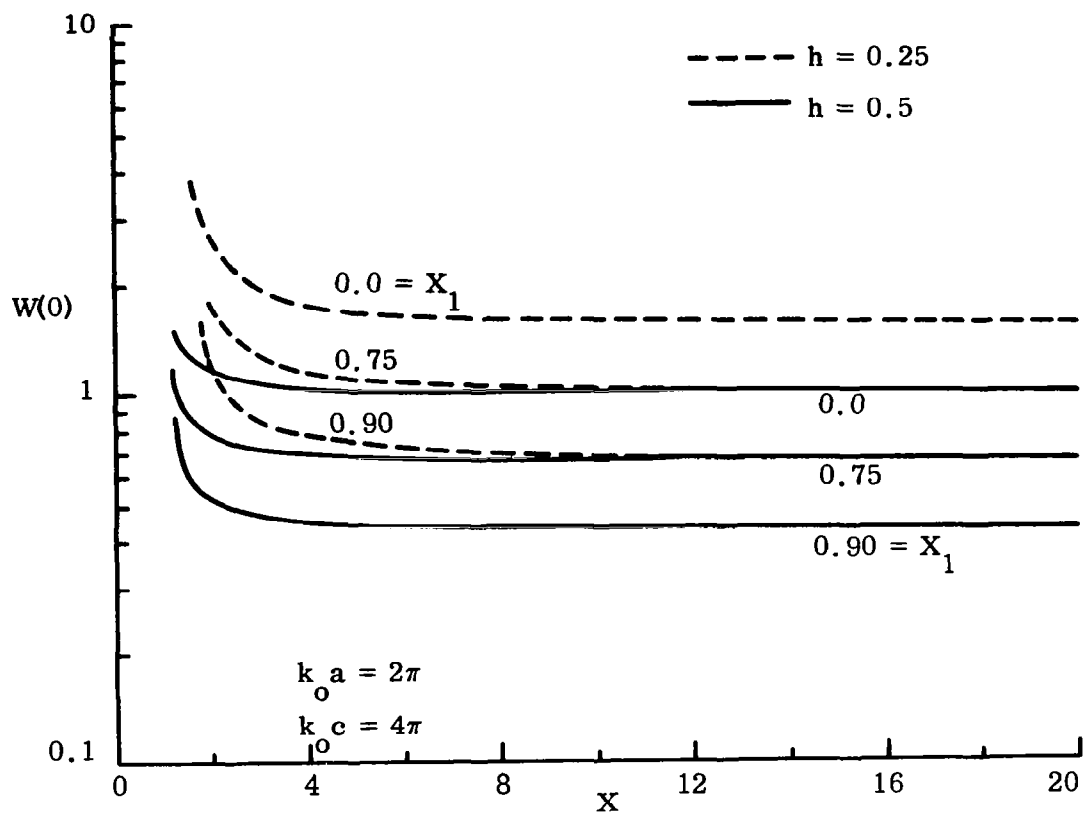
FIG. 3.8: NORMALIZED RADIATION IN FORWARD DIRECTION FOR THE SLOTTED PLASMA SHEATH AS A FUNCTION OF X. THE PARAMETERS ARE X_1 AND h.

When the plasma slot is opened above such a minimum only a weak coupling of
the power into the slot waveguide will result. Opening the slot above a
field maximum will give large coupling.   In effect this type of analysis
was carried out by Olte(1965) when the slotted plasma sheath was replaced
by a perfectly conducting slotted shell. Extension of this type of analysis
to the thick slotted plasma sheath remains to be done.

IV

CONCLUSIONS

The radiation through a plasma sheath of a magnetic line source excited cylinder of infinite conductivity is formulated using the vector Green's theorem and the external Green's function of the cylinder. The magnetic field is along the axis of the cylinder while the electric field is entirely transverse to the cylinder. A two dimensional singular integral equation is formulated for the plasma current, assuming it satisfies the Ohm's law. However, the solution of the integral equation is not readily obtainable. Some approximate plasma current representations are suggested, more or less on physical grounds, to study the effect of underdense plasma sheath on the cylindrical antenna radiation fields. The plasma sheath may contain a slot.

For the overdense plasma sheath, provided the leakage through it may be neglected in comparison with the radiation through the plasma slot, we may introduce plasma waveguide considerations in the analysis. When some minimal parameter restrictions are met, the plasma slot will support propagating transverse magnetic waves. The wave analysis becomes elementary when the slot walls are parallel. The lower order mode then is a perturbation of the transverse electromagnetic mode. The radiation analysis is particularly simple when only this mode is propagating. In the above case we carry out the analysis for the plasma sheath closely fitting the cylinder, and the parallel face plasma slot being centered above the magnetic line source. The calculations consider loss-less plasma, with the plasma

47

slot width of 1/4 and 1/2 free space wavelength, and show that the radiation in the forward direction is re-established or slightly increased for zero plasma frequency in the slot, moderate loss is incurred as the plasma frequency in the slot approaches the angular field frequency. If the plasma frequency in the slot exceeds the angular field frequency, but still being less than the plasma frequency in the remainder of the sheath, a very severe attenuation of radiation will result.

The gain function of the slot in a 4 wavelength diameter plasma sheath has a broad forward lobe, the 3 db points being 156° wide for 1/4 wave slot and 112° wide for a 1/2 wave slot. The back lobes are no more than 20 db down from the radiation in the forward direction. The significant back radiation results from the surface waves that are supported by the external plasma sheath surface.

THE FIELDS OF A MAGNETIC LINE SOURCE IN THE PRESENCE OF A PERFECTLY
CONDUCTING   CYLINDER

In this appendix we review the two dimensional problem of an axial

magnetic line source radiation in the presence of a perfectly conducting

cylinder of radius a, as shown in Figure A-1. The line source is located

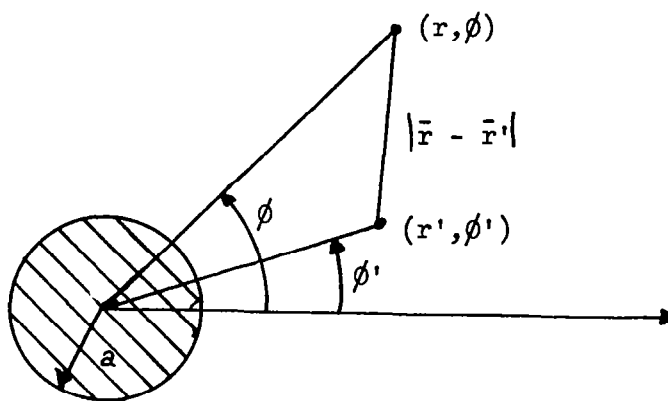by coordinates (r', ϕ'), and the field point is denoted by the coordinates

Fig. A-1:   The Configuration.

(r,ϕ). The z-axis of the cylindrical coordinates coincides with the perfect-
ly conducting cylinder axis.

Employing the rationalized MKS units and assuming $e^{j\omega t}$ time dependence

for all field quantities, one can show (for example, Harrington 1961) that

the magnetic field from the magnetic line source in free space is given by

$$H_z^{(i)} = - \frac{k_o^2}{4\omega\mu_o} I_m H_o^{(2)}(k_o|\bar{r} - \bar{r}'|) \qquad (A-1)$$

where $k_o = \omega\sqrt{\mu_o\epsilon_o}$, and I_m is the amplitude of the magnetic current filament. When we consider $H_z^{(i)}$ as the field incident on the cylinder, then the magnetic field scattered by the cylinder is denoted by

$$H_z^{(s)} = -\frac{k_o^2}{4\omega\mu_o}\, I_m \sum_{n=-\infty}^{\infty} a_n H_n^{(2)}(k_o r') H_n^{(2)}(k_o r) e^{jn(\phi-\phi')}. \tag{A-2}$$

Expanding the incident magnetic field by the addition theorem for the cylindrical functions and using the orthogonality properties of the circular functions, we are able to identify the unknown coefficients a_n from the boundary condition

$$-\frac{\partial}{\partial r}\left[H_z^{(i)} + H_z^{(s)}\right] = 0 \text{ at } r = a \tag{A-3}$$

as

$$a_n = -\frac{J_n'(k_o a)}{H_n^{(2)'}(k_o a)}. \tag{A-4}$$

The total magnetic field (incident and scattered) we may now write as

$$H_z(r,\phi) = \frac{k_o^2}{4\omega\mu_o}\, I_m \left\{ -H_o^{(2)}\left(k_o\sqrt{r^2 + r'^2 - 2rr'\cos(\phi-\phi')}\right) + \right.$$

$$\left. \sum_{n=0}^{\infty} c_n \frac{J_n'(k_o a)}{H_n^{(2)'}(k_o a)} H_n^{(2)}(k_o r') H_n^{(2)}(k_o r) \cos n(\phi-\phi') \right\} \tag{A-5}$$

where $c_n = 1$ for $n = 0$; $c_n = 2$ for $n = 1,2,3,\cdots$.

The electric fields can be derived by differentiation from (A-5); they are:

50

$$E_r(r,\phi) = \frac{1}{j\omega\epsilon_o r} \frac{\partial}{\partial\phi} H_z(r,\phi) \qquad (A-6)$$

$$E_\phi(r,\phi) = -\frac{1}{j\omega\epsilon_o} \frac{\partial}{\partial r} H_z(r,\phi) \quad . \qquad (A-7)$$

We may place the magnetic line source on the perfectly conducting cylinder by letting $r' \longrightarrow a$. The fields then assume a particularly simple form:

$$H_z(r,\phi) = \frac{jk_o}{2\pi a\omega\mu_o} I_m \sum_{n=0}^{\infty} c_n \frac{H_n^{(2)}(k_o r)}{H_n^{(2)'}(k_o a)} \cos n\,(\phi - \phi') \qquad (A-8)$$

$$E_r(r,\phi) = -\frac{1}{2\pi k_o a} I_m \sum_{n=0}^{\infty} \frac{n}{r} c_n \frac{H_n^{(2)}(k_o r)}{H_n^{(2)'}(k_o a)} \sin n\,(\phi - \phi') \qquad (A-9)$$

$$E_\phi(r,\phi) = -\frac{1}{2\pi a} I_m \sum_{n=0}^{\infty} c_n \frac{H_n^{(2)'}(k_o r)}{H_n^{(2)'}(k_o a)} \cos n\,(\phi - \phi') \quad . \qquad (A-10)$$

The exciting voltage of the cylinder is defined by

$$V = -\int_0^{2\pi} E_\phi(a,\phi) a \, d\phi \quad . \qquad (A-11)$$

Substituting (10) in (11) and performing the integration, we obtain

$$V = I_m \quad , \qquad (A-12)$$

and indeed magnetic current is measured in volts.

APPENDIX   B

CONCENTRIC PLASMA SHEATH OF UNIFORM DENSITY ENCLOSING A MAGNETIC LINE SOURCE EXCITED PERFECTLY CONDUCTING CYLINDER

We consider the configuration as shown in Fig. B-1, and take the free space permeability μ_o and the free space permittivity ϵ_o to apply for all radii. The z-axis of the cylindrical coordinate system (r,φ,z) is coincident with the perfectly conducting cylinder axis. The magnetic line source on the perfectly conducting cylinder surface is accounted for by

$$E_\varphi(a,\varphi) = - V \frac{\delta(\varphi_s - \varphi)}{a} \quad , \tag{B-1}$$

the time dependence $e^{j\omega t}$ being suppressed. The field quantities are independent of z and hence the magnetic field may be represented by

$$H_z(r,\varphi) = \sum_{m=-\infty}^{\infty} [A_m J_m(k_o r) + B_m N_m(k_o r)]e^{jm\varphi}, \quad a<r<b, \tag{B-2a}$$

$$= \sum_{m=-\infty}^{\infty} [C_m J_m(kr) + D_m N_m(kr)]e^{jm\varphi}, \quad b<r<c, \tag{B-2b}$$

$$= \sum_{m=-\infty}^{\infty} F_m H_m^{(2)}(k_o r)e^{jm\varphi}, \quad c < r, \tag{B-2c}$$

where $k_o = \omega\sqrt{\mu_o\epsilon_o}$ and $k = k_o\sqrt{1-j\sigma/(\omega\epsilon_o)}$. From the Maxwell's equations we obtain that the electric field $E_r(r,\varphi)$ is given by differention of (B-2) according to (A-6), and the electric field $E_\varphi(r,\varphi)$ according to (A-7). We only note that for $b<r<c$ one should substitute $\epsilon = \epsilon_o - j\frac{\sigma}{\omega}$
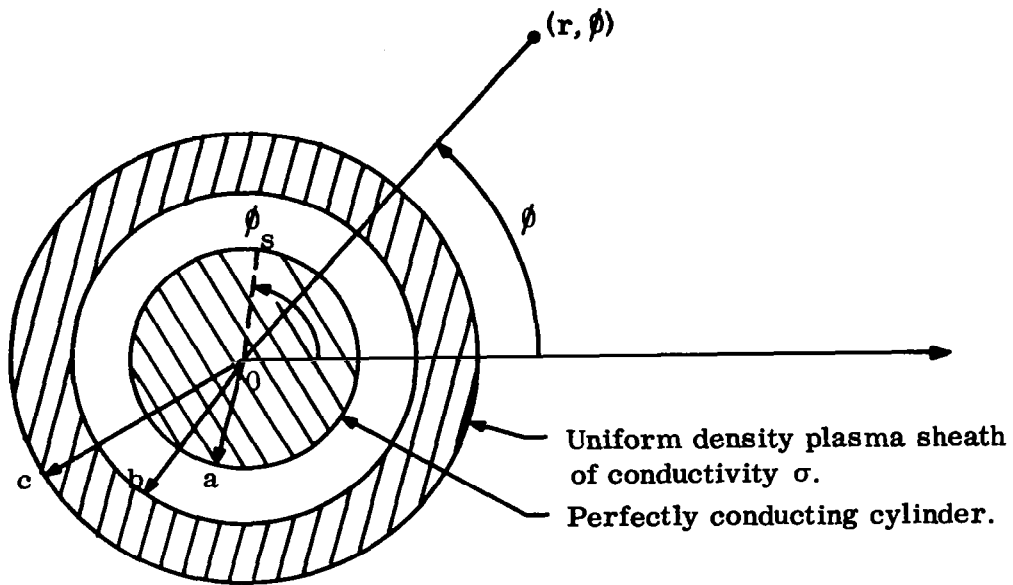
FIG. B.1: MAGNETIC LINE SOURCE EXCITED CYLINDER ENCLOSED
BY A PLASMA SHEATH.

for ϵ_o in (A-6) and (A-7).

From (B-1) and from the continuity of $E_\varphi(r,\varphi)$ and $H_z(r,\varphi)$ at $r = b,c$, by applying the orthogonality properties of the circular functions we obtain

$$
\begin{bmatrix}
J_m(k_o b) & N_m(k_o b) & -J_m(kb) & -N_m(kb) & 0 \\
\epsilon' J'_m(k_o b) & \epsilon' N'_m(k_o b) & -k' J'_m(kb) & -k' N'_m(kb) & 0 \\
J'_m(k_o a) & N'_m(k_o a) & 0 & 0 & 0 \\
0 & 0 & J_m(kc) & N_m(kc) & -H_m^{(2)}(k_o c) \\
0 & 0 & k' J'_m(kc) & k' N'_m(kc) & -\epsilon H_m^{(2)'}(k_o c)
\end{bmatrix}
\begin{bmatrix}
A_m \\
B_m \\
C_m \\
D_m \\
F_m
\end{bmatrix}
=
\begin{bmatrix}
0 \\
0 \\
\dfrac{j\omega\epsilon_o V}{2\pi k_o a} e^{-jm\varphi_s} \\
0 \\
0
\end{bmatrix}
$$

where k' and k/k_o, and $\epsilon' = 1 - j\dfrac{\sigma}{\omega\epsilon_o}$. $\hspace{2cm}$ (B-3)

We compute the determinant of (B-3)

$$\Delta_m = k'^2 H_m^{(2)}(k_o c)[N'_m(kc)J'_m(kb) - J'_m(kc)N'_m(kb)] \cdot [J_m(k_o b)N_m(k_o a) - J'_m(k_o a)N_m(k_o b)]$$

$$-k'\epsilon \left\{ H_m^{(2)}(k_o c)[N'_m(kc)J_m(kb) - J'_m(kc)N_m(kb)] \cdot [J'_m(k_o b)N'_m(k_o a) - J'_m(k_o a)N'_m(k_o b)] \right.$$

$$\left. + H_m^{(2)'}(k_o c)[N_m(kc)J'_m(kb) - J_m(kc)N'_m(kb)] \cdot [J_m(k_o b)N'_m(k_o a) - J'_m(k_o a)N_m(k_o b)] \right\}$$

$$+\epsilon'^2 H_m^{(2)'}(k_o c)[J_m(k b)N_m(kc) - J_m(kc)N_m(kb)] \cdot [J_m(k_o b)N'_m(k_o a) - J'_m(k_o a)N'_m(k_o b)]$$

$$\hspace{12cm} (B-4)$$

and those coefficients of interest in this study C_m, D_m, and F_m, i.e.,

$$\Delta_m C_m = \frac{j\omega\epsilon_o V}{(\pi k_o)^2 ab} N_m e^{-jm\varphi_s} \hspace{2cm} (B-5)$$

$$\Delta_m D_m = - \frac{j\omega\epsilon_o V}{(\pi k_o)^2 \, ab} \, M_m \, e^{-jm\varphi_s} \tag{B-6}$$

$$\Delta_m F_m = \frac{2j\omega\epsilon V}{(\pi k_o)^3 \, abc} \, e^{-jm\varphi_s} \tag{B-7}$$

where

$$N_m = -\epsilon'^2 N_m(kc) \, H_m^{(2)'}(k_o c) + k'\epsilon' N_m'(kc) \, H_m^{(2)}(k_o c) \tag{B-8}$$

$$M_m = -\epsilon'^2 J_m(kc) \, H_m^{(2)'}(k_o c) + k'\epsilon' J_m'(kc) \, H_m^{(2)}(k_o c) \ . \tag{B-9}$$

We compute the φ- component of electric current density in the plasma,

$$i_\varphi(r,\varphi) = \sigma \, E_\varphi(r,\varphi)$$

$$= \frac{\sigma k \epsilon_o \, V}{(\pi k_o)^2 \, \epsilon \, ab} \, \sum_{m=0}^{\infty} c_m \, I_m^{(\varphi)}(r) \, \cos m \, (\varphi - \varphi_s) \tag{B-10}$$

where

$$I_m^{(\varphi)}(r) = [-N_m J_m'(kr) + M_m N_m'(kr)] \, \Delta_m^{-1} \ , \tag{B-11}$$

and the r-components of electric current density,

$$i_r(r,\varphi) = \sigma \, E_r(r,\varphi)$$

$$= \frac{j2\sigma\epsilon_o \, V}{(\pi k_o)^2 \, \epsilon \, ab} \, \sum_{m=1}^{\infty} \frac{m}{r} \, I_m^{(r)}(r) \, \sin m \, (\varphi - \varphi_s) \ , \tag{B-12}$$

where

$$I_m^{(r)}(r) = [N_m J_m(kr) - M_m N_m(kr)] \Delta_m^{-1} \quad . \tag{B-13}$$

The magnetic field outside the plasma sheath, $r > c$,

$$H_z(r,\varphi) = \frac{2j\omega\epsilon V}{(\pi k_o)^3 abc} \sum_{m=0}^{\infty} \frac{c_m}{\Delta_m} H_m^{(2)}(k_o r) \cos m (\varphi - \varphi_s) \quad . \tag{B-14}$$

REFERENCES

Den, C-F. (1966), "Impedance of a Wedge Excited Coaxial Antenna with a Plasma Sheath", University of Michigan Radiation Laboratory Report 5825-9-T, 1966.

Harrington, Roger F., (1961), *Time-Harmonic Electromagnetic Fields*, McGraw-Hill Book Co., p 237.

Olte, A., (1964), Y. Hayashi, "On the Antenna Radiation Through a Plasma Sheath", University of Michigan Radiation Laboratory Report 5825-1-F, June, 1964.

Olte, A. (1965), "Radiation of an Elementary Cylinder Antenna Through a Slotted Enclosure", *IEEE Trans. on Antennas and Propagation*, Vol. AP-13, No. 5, September, 1965.

Olte, A. (1965), "The Radiation Pattern of an Electric Line Current Enclosed by an Axially Slotted Plasma Sheath-I," University of Michigan Radiation Laboratory Report 5825-4-T, November, 1965.

Olte, A. (1966), "The Radiation Pattern of an Electric Line Current Enclosed by an Axially Slotted Plasma Sheath-II," University of Michigan Radiation Laboratory Report 5825-6-T, February, 1966.

ACKNOWLEDGEMENT

NASA-Langley, 1967 CR-677